in vitro (Fig. 3). By using the genes commonly up-regulated both *in vivo* and *in vitro*, PCA was performed for 32 compounds, and principal component 1 was identified as a convenient parameter to extract PPARα agonists from the database (Fig. 3). This study is one of the first to create an *in vivo–in vitro* bridge for the validation of a genomic biomarker.

4.6 Bridging between the rat and human: Coumarin-induced hepatotoxicity [19]

A system that perfectly predicts hepatotoxicity in the rat would not necessarily improve the prediction of hepatotoxicity in humans. The final goal must be the prediction of hepatotoxicity in humans for drug development. The extrapolation of toxicity data from rodent to human is not sufficient. However, if general toxic mechanisms or toxicological pathways are conserved over species, they would be useful bridges between animal models and clinical events. One expected result from toxicogenomics technology is to overcome the barrier due to species difference in the prediction of clinical toxicity.

We investigated the possibility of an informational bridge connecting transcript responses between rat and human hepatocytes, and rat liver *in vivo* after the administration of coumarin. In this experiment, primary cultured rat hepatocytes were exposed to 12, 60, and 300 μM coumarin for 24 h. No obvious cytotoxicity was detected by LDH release (100.5, 97.7, and 95.1% of control, respectively). Then, we extracted the significant genes according to the gene list obtained from *in vivo* study; the extracted genes showed

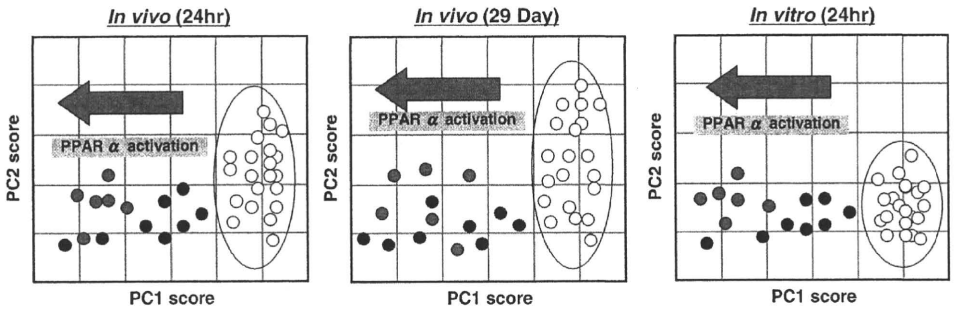

Figure 3. An *in vivo – in vitro* bridge for genomic biomarkers to assess PPARα agonistic action. A model case for creating an *in vivo – in vitro* bridge for genomic biomarkers is presented. The data from three agonists of PPARα in our database (clofibrate, WY-14 643 and gemfibrozil) were analyzed, and 41 commonly up-regulated probe sets between *in vivo* and *in vitro* were extracted. The validity of these probe sets as biomarkers for the evaluation of PPARα agonistic activity was evaluated by PCA. These plots show the principal separation of samples due to putative PPARα agonistic activity toward the negative direction on the *x*-axis, PC1.

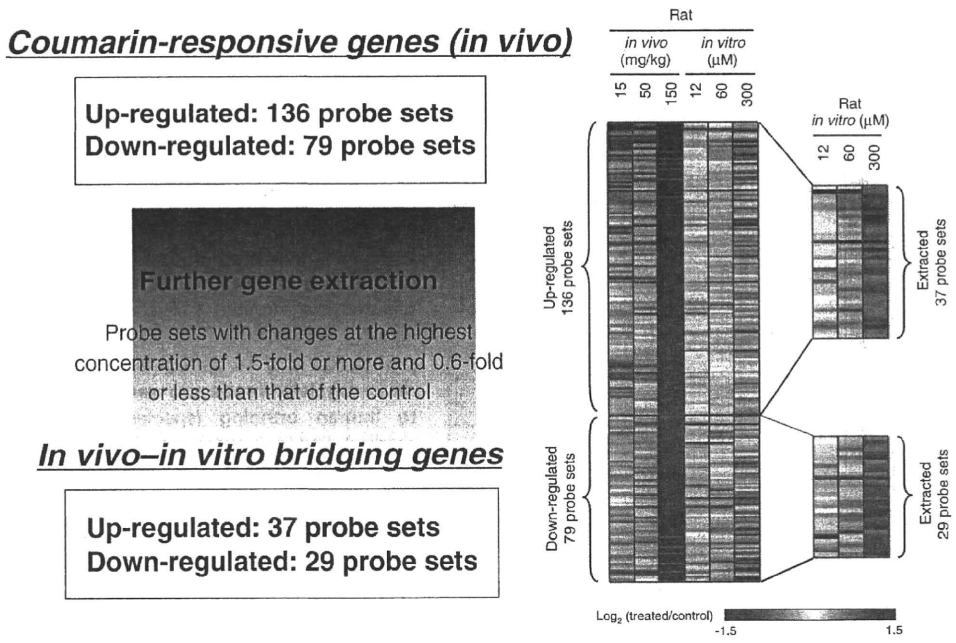

Figure 4. Heat map of the expression profiles of probe sets in rat liver and rat hepatocytes treated with coumarin. A considerable number of the *in vivo*-selected probe sets show similar profiles between *in vivo* and *in vitro* assays. The selected genes, namely the *in vivo – in vitro* bridging probes, had clear dose-dependent changes in expression.

significant up-regulation (136 probe sets) or down-regulation (79 probe sets) in livers treated with 150 mg/kg coumarin. A similar trend was observed between *in vivo* and *in vitro* cell responses, although the extent of the response (the fold change) was generally smaller, and fewer genes showed a measurable change in the *in vitro* cell assay (Fig. 4). Probe sets showing changes of 1.5-fold or more or 0.6-fold or less than that of the control at the highest concentration (300 μM) in rat hepatocytes were selected as *in vivo–in vitro* bridging probes that reflect the toxicological mechanism of coumarin *in vivo*. The selected genes (37 up-regulated and 29 down-regulated) had clear dose-dependent changes in expression that enabled us to assess the hepatotoxicity of coumarin by using the *in vitro* data (Fig. 4).

Next, cultured human hepatocytes were exposed to 12, 60, and 300 μM coumarin for 24 h. No obvious cytotoxicity was detected by LDH release (100.6, 100.9, and 102.0% of control, respectively). The *in vivo–in vitro* bridging probes were assigned to their human ortholog genes to form a set of rat–human bridging probes, and changes in their expression were compared in rat *versus* human hepatocytes. In total, 14 up-regulated probe sets and 11 down-regulated probe sets were identified; their relative expression levels are shown in Fig. 5. The pattern of changes in gene expression was similar in rat and human cells, but the extent of the changes was more prominent in rat cells than in human cells, in accordance with the known species-specific difference in hepatotoxicity [32–38]. In the case of diclofenac, which is a hepatotoxicant without species difference, there was no evidence of a species-specific difference in gene expression between rat and human cells. The observation that the induction of stress-related genes was more robust in rat cells than in human cells could be a direct reflection of the extent of stress and subsequent damage caused by coumarin in each species. Although more data are needed to connect species and model systems with human risk assessment, this approach is an important step in bridging the differences between species.

5 Future perspectives

This review focuses on our efforts in toxicogenomics research and highlights recent progress in the application of toxicogenomics. In the early stage of drug development, genomic biomarkers are used to identify and optimize lead compounds among several candidates. As full-scale toxicity testing is quite costly, safety assessment of candidate drugs is usually performed just before the clinical trial. If serious toxicity emerges at this stage, it might be necessary to return to the screening of seed compounds, because toxicity is often inherent to the basic structure and is thus never eliminated by minor modification. If the potential phenotype (when repeatedly dosed) is predictable in the early stage

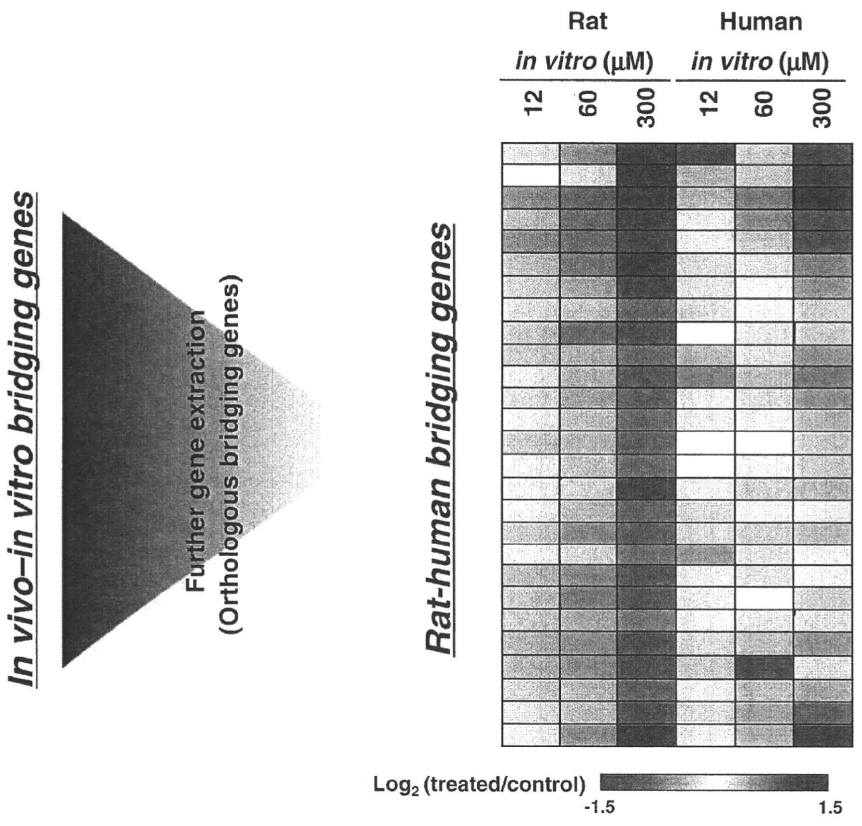

Figure 5. Heat map of the expression profile of probe sets in rat and human hepatocytes treated with coumarin. Among the *in vivo* – *in vitro* bridging probes for rats, 14 up-regulated and 11 down-regulated probe sets were assigned to human ortholog (species bridging marker), and their expression is shown as a heat map of the expression profile in rat and human hepatocytes treated with coumarin (12, 60 and 300 μM). Each probe set dose-dependently responded to coumarin in both species, whereas the extent of the changes appears to be more prominent in rats than in humans.

of drug development by gene expression data from a small number of experimental animals, it would effectively cut the time and cost of drug development. The use of genomic biomarkers in the early stage of drug development will strengthen the safety screening of drug candidates before they are administered to humans. The use of genomic biomarkers will also reduce the number of animals sacrificed during drug development. However, the candidate biomarkers reviewed here have not necessarily been evaluated with large independent test sets and are rarely validated across laboratories. Further definitive validation studies are absolutely essential for judging the acceptability of candidate genomic biomarkers in pre-clinical safety assessments. Furthermore, regulatory agencies, the pharmaceutical industry and academia must establish guidelines for the integration of "omics" data, including toxicogenomics and genomic biomarkers, into drug safety assessment. We are currently in the project's second stage, known as the TGP2. Our goals are as follows: (i) establishment of genomic biomarkers to predict the toxicity of drug candidates in the early stage of drug development, (ii) bridging of species differences, and (iii) application of toxicogenomic data for regulatory science. These efforts will contribute to the accelerated development of more effective and safer drugs.

The PSTC also represents a next important step in the validation and regulatory use of new pre-clinical biomarker tests with the initiative of the C-Path Institute. The novel biomarkers are internally developed and used by each individual pharmaceutical company and consortium are of limited value for regulatory use because the methods used have not been validated by an independent party. To resolve these issues, there is a growing need for a large and cross-institutional study on a global scale. The PSTC is a public–private partnership, led by the C-Path Institute, which brings together pharmaceutical companies to share and validate each other's safety testing methods under advisement of the Food and Drug Administration (FDA) and its European counterpart, the European Medicines Evaluation Agency (EMEA). The aim of the PSTC is to identify and qualify safety biomarkers for regulatory use as part of the Food and Drug Administration's Critical Path Initiative. The 17 corporate members of the consortium share internally developed pre-clinical safety biomarkers in five workgroups: carcinogenicity, kidney, liver, muscle, and vascular injury. Consortium members are sharing their new pre-clinical biomarker tests for examination and cross-validation by other members of the consortium. Candidate genomic biomarkers reviewed here will need a similar validation process through collaborative research like that of PSTC. These processes are expected to enable the regulatory agencies to write new guidelines for industry that identify more accurate methods to predict drug safety.

The authors have declared no conflict of interest.

6 References

[1] Ismail, K., Landis, J., Can the pharmaceutical industry reduce attrition rates? *Nat. Rev. Drug Discov.* 2003, *3*, 711–715.

[2] Edgar, R., Domrachev, M., Lash, A. E., Gene expression omnibus: NCBI gene expression and hybridization array data repository. *Nucleic Acids Res.* 2002, *30*, 207–210.

[3] Barrett, T., Troup, D. B., Wilhite, S. E., Ledoux, P. *et al.*, NCBI GEO: archive for high-throughput functional genomic data. *Nucleic Acids Res.* 2009, *37*, D885–D890.

[4] Brazma, A., Parkinson, H., Sarkans, U., Shojatalab, M. *et al.*, ArrayExpress – a public repository for microarray gene expression data at the EBI. *Nucleic Acids Res.* 2003, *31*, 68–71.

[5] Parkinson, H., Kapushesky, M., Kolesnikov, N., Rustici, G. *et al.*, ArrayExpress update – from an archive of functional genomics experiments to the atlas of gene expression. *Nucleic Acids Res.* 2009, *37*, D868–D872.

[6] Ikeo, K., Ishi-i, J., Tamura, T., Gojobori, T. *et al.*, CIBEX: center for information biology gene expression database. *C. R. Biol.* 2003, *326*, 1079–1082.

[7] Hayes, K. R., Vollrath, A. L., Zastrow, G. M., McMillan, B. J. *et al.*, EDGE: a centralized resource for the comparison, analysis, and distribution of toxicogenomic information. *Mol. Pharmacol.* 2005, *67*, 1360–1368.

[8] Waters, M., Stasiewicz, S., Merrick, B. A., Tomer, K. *et al.*, CEBS Chemical Effects in Biological Systems: a public data repository integrating study design and toxicity data with microarray and proteomics data. *Nucleic Acids Res.* 2008, *36*, D892–D900.

[9] Burgoon, L. D., Zacharewski, T. R., dbZach toxicogenomic information management system. *Pharmacogenomics* 2007, *8*, 287–291.

[10] Mattingly, C. J., Colby, G. T., Forrest, J. N., Boyer, J. L., The Comparative Toxicogenomics Database (CTD). *Environ. Health Perspect.* 2003, *111*, 793–795.

[11] Mattingly, C. J., Rosenstein, M. C., Colby, G. T., Forrest, Jr, J. N. *et al.*, The Comparative Toxicogenomics Database (CTD): a resource for comparative toxicological studies. *J. Exp. Zoolog. A Comp. Exp. Biol.* 2006, *305*, 689–692.

[12] Mulrane, L., Rexhepaj, E., Smart, V., Callanan, J. J. *et al.*, Creation of a digital slide and tissue microarray resource from a multi-institutional predictive toxicology study in the rat: an initial report from the PredTox group. *Exp. Toxicol. Pathol.* 2008, *60*, 235–245.

[13] McBurney, R. N., Hines, W. M., Von Tungeln, L. S., Schnackenberg, L. K. *et al.*, The liver toxicity biomarker study: phase I design and preliminary results. *Toxicol. Pathol.* 2009, *37*, 52–64.

[14] Porter, M. W., Castle, A. L., Orr, M. S., Mendrick, D. L., in: Burczynski, M. E. (Ed.), *Predictive Toxicogenomics: An Introduction to Toxicogenomics*, CRC Press, Boca Raton 2003, pp. 225–260.

[15] Tibshirani, R., Hastie, T., Narasimhan, B., Chu, G., Diagnosis of multiple cancer types by shrunken centroids of gene expression. *Proc. Natl. Acad. Sci. USA* 2002, *99*, 6567–6572.

[16] Brown, M. P., Grundy, W. N., Lin, D., Cristianini, N. *et al.*, Knowledge-based analysis of microarray gene expression data by using support vector machines. *Proc. Natl. Acad. Sci. USA* 2000, *97*, 262–267.

[17] Kiyosawa, N., Shiwaku, K., Hirode, M., Omura, K. *et al.*, Utilization of a one-dimensional score for surveying chemical-induced changes in expression levels of multiple biomarker gene sets using a large-scale toxicogenomics database. *J. Toxicol. Sci.* 2006, *31*, 433–448.

[18] Uehara, T., Kiyosawa, N., Hirode, M., Omura, K. *et al.*, Gene expression profiling of methapyrilene-induced hepatotoxicity in rat. *J. Toxicol. Sci.* 2008, *33*, 37–50.

[19] Uehara, T., Kiyosawa, N., Shimizu, T., Omura, K. *et al.*, Species-specific differences in coumarin-induced hepatotoxicity as an example toxicogenomics-based approach to assessing risk of toxicity to humans. *Hum. Exp. Toxicol.* 2008, *27*, 23–35.

[20] Kiyosawa, N., Uehara, T., Gao, W., Omura, K. *et al.*, Identification of glutathione depletion-responsive genes using phorone-treated rat liver. *J. Toxicol. Sci.* 2007, *32*, 469–486.

[21] James, L. P., Mayeux, P. R., Hinson, J. A., Acetaminophen-induced hepatotoxicity. *Drug Metab. Dispos.* 2003, *31*, 1499–1506.

[22] Kiyosawa, N., Ito, K., Sakuma, K., Niino, N. *et al.*, Evaluation of glutathione deficiency in rat livers by microarray analysis. *Biochem. Pharmacol.* 2004, *68*, 1465–1475.

[23] Hirode, M., Ono, A., Miyagishima, T., Nagao, T. *et al.*, Gene expression profiling in rat liver treated with compounds inducing phospholipidosis. *Toxicol. Appl. Pharmacol.* 2008, *229*, 290–299.

[24] Hirode, M., Horinouchi, A., Uehara, T., Ono, A. *et al.*, Gene expression profiling in rat liver treated with compounds inducing elevation of bilirubin. *Hum. Exp. Toxicol.* 2009, *28*, 231–244.

[25] Uehara, T., Hirode, M., Ono, A., Kiyosawa, N. *et al.*, A toxicogenomics approach for early assessment of potential non-genotoxic hepatocarcinogenicity of chemicals in rats. *Toxicology* 2008, *250*, 15–26.

[26] Ellinger-Ziegelbauer, H., Gmuender, H., Bandenburg, A., Ahr, H. J., Prediction of a carcinogenic potential of rat hepatocarcinogens using toxicogenomics analysis of short-term *in vivo* studies. *Mutat. Res.* 2008, *637*, 23–39.

[27] Ellinger-Ziegelbauer, H., Stuart, B., Wahle, B., Bomann, W., Ahr, H. J., Comparison of the expression profiles induced by genotoxic and nongenotoxic carcinogens in rat liver. *Mutat. Res.* 2005, *575*, 61–84.

[28] Fielden, M. R., Brennan, R., Gollub, J., A gene expression biomarker provides early prediction and mechanistic assessment of hepatic tumor induction by nongenotoxic chemicals. *Toxicol. Sci.* 2007, *99*, 90–100.

[29] Nie, A. Y., McMillian, M., Parker, J. B., Leone, A. *et al.*, Predictive toxicogenomics approaches reveal underlying molecular mechanisms of nongenotoxic carcinogenicity. *Mol. Carcinog.* 2006, *45*, 914–933.

[30] Fielden, M. R., Nie, A., McMillian, M., Elangbam, C. S., Interlaboratory evaluation of genomic signatures for predicting carcinogenicity in the rat. *Toxicol. Sci.* 2008, *103*, 28–34.

[31] Tamura, K., Ono, A., Miyagishima, T., Nagao, T. *et al.*, Profiling of gene expression in rat liver and rat primary cultured hepatocytes treated with peroxisome proliferators. *J. Toxicol. Sci.* 2006, *31*, 471–490.

[32] Vassallo, J. D., Hicks, S. M., Daston, G. P., Lehman-McKeeman, L. D., Metabolic detoxification determines species differences in coumarin-induced hepatotoxicity. *Toxicol. Sci.* 2004, *80*, 249–257.

[33] Felter, S. P., Vassallo, J. D., Carlton, B. D., Daston, G. P., A safety assessment of coumarin taking into account species-specificity of toxicokinetics. *Food Chem. Toxicol.* 2006, *44*, 462–475.

[34] Vassallo, J. D., Hicks, S. M., Daston, G. P., Lehman-McKeeman, L. D., Metabolic detoxification determines species differences in coumarin-induced hepatotoxicity. *Toxicol. Sci.* 2004, *80*, 249–257.

[35] Felter, S. P., Vassallo, J. D., Carlton, B. D., Daston, G. P., A safety assessment of coumarin taking into account species-specificity of toxicokinetics. *Food Chem. Toxicol.* 2006, *44*, 462–475.

[36] Born, S. L., Hu, J. K., Lehman-McKeeman, L. D., o-Hydroxyphenylacetaldehyde is a hepatotoxic metabolite of coumarin. *Drug Metab. Dispos.* 2000, *28*, 218–223.

[37] Born, S. L., Caudill, D., Smith, B. J., Lehman-McKeeman, L. D., *In vitro* kinetics of coumarin 3,4-epoxidation: application to species differences in toxicity and carcinogenicity. *Toxicol. Sci.* 2000, *58*, 23–31.

[38] Lake, B. G., Investigations into the mechanism of coumarin-induced hepatotoxicity in the rat. *Arch. Toxicol.* 1984, *7*, 16–29.

日薬理誌（*Folia Pharmacol. Jpn.*）**136**，●～●（2010）

トランスレーショナルリサーチ④
創薬
シリーズ(5)

トキシコゲノミクスプロジェクトと安全性試験

漆谷　徹郎

要約：マイクロアレイ技術の発達により，一度に全遺伝子の発現を定量するという，一時代前は夢のようなことが可能となった．医薬品開発における安全性研究は，何が起こるか分からないという状態で発生確率の低い有害作用の可能性を予測せよという，一見して不可能なことを強いられていたが，これを毒性学に応用したトキシコゲノミクスという領域が生まれ，安全性研究に革命をもたらした．我が国のトキシコゲノミクスプロジェクトは，世界最大規模のデータベースTG-GATEsを完成させたが，これを安全性試験に適用するには多くの課題が見いだされてきた．現在，後継プロジェクトにおいて，このシステムを活用し，安全性バイオマーカーの創出に力を注いでいる．

はじめに

ポストゲノム時代といわれる現在，新薬のシーズを見いだす技術は飛躍的に発展を遂げているようにみえるものの，日本のみならず世界的に新規薬物の成功例はかえって減少しつつある．ヒトゲノムプロジェクトとそれに続く各種生物のゲノム解読は，医学・生理学・生物学の進歩に大きく貢献したことは明らかであるが，その進歩が新薬開発に直結していないという感がある．

前世紀の薬物開発は，モデル動物に人為的に作り出した症状を指標にしてスクリーニングすることが多く，臨床に持っていって初めて，ヒトには無効な「ラットのための良薬を作ってしまった」ことが判明する場合が見られた．ヒトゲノムの解明は「疾患関連遺伝子」という標的に対する薬物開発を可能とした．従って少なくとも試験管レベルではヒトに対して有効性を示す薬物を選択することが可能となっている．それにもかかわらず多くの候補化合物がドロップアウトしているのは，そのかなりの部分が非臨床試験において見いだせなかった毒性が臨床において発現したためといってよい(1)．これは製薬産業の開発コスト高を招き，医療費の圧迫を招くばかりでなく，「有害な化合物で人体実験をした結果，使用できないことが判明した」という，倫理的にも大きな問題を生み出すことになる．綿密な安全性試験を行っても臨床での安全性予測の確度が低いと言うことは，逆の見方をすると，本来は臨床で有用であったはずの新薬を，毒性ありとして葬り去った例があったかもしれない．

1．安全性試験の問題点

現在の安全性試験は，過去の幾多の事例の反省の上に立ち，実験動物やデータ管理に関してソフト・ハードの両面から強力な標準化を推し進め，その質の向上は著しい．しかし，試験データ自身の信頼性向上は，必ずしも臨床での安全性予測の信頼性向上を意味するものではない．薬物自身が目的とする薬理作用の延長上に明らかな臓器・細胞毒性がある場合は，その薬物の用量反応関係から，薬用量における有害作用発現程度が予測でき，対処しやすい．一方，実際の臨床上問題になる副作用に関しては，薬理作用の延長である場合は少なく，代謝物など薬物それ自身の作用ですらない場合も多い．また，仮に重大な副作用が臨床用量で数千～数万分の1の確率で発生したとすれば，そのような薬物は発売中止せざるを得ないが，これを動物実験で予測しようとすると，たとえ種差がなくても，数千例の実験でも不足であるという，非現実的なことになる．そして勿論，種の壁は厚い．現実の安全性試験は「実験動物に極端な高用量を与えたときに見えてくる病態生理学的変化を，ヒトにおいて薬用量で低頻度に生じる有害作用へ外挿する」という，原理的にみても困難な戦略をとらざるを得ない．

「予測不能な毒性を予測する」という逆説を打破するために考えられる最も強力な戦略の一つが，「生体に薬物が作用する時に生じるすべての遺伝子発現変化

キーワード：オミクステクノロジー，マイクロアレイ，データベース
同志社女子大学薬学部（〒610-0395 京都府京田辺市興戸）　E-mail: turushid@dwc.doshisha.ac.jp
(独)医薬基盤研究所 トキシコゲノミクス・インフォマティクスプロジェクト（〒567-0085 大阪府茨木市彩都あさぎ7-6-8）
原稿受領日：2010年3月23日，依頼原稿
Title: The Toxicogenomics Project and drug safety evaluation.　Author: Tetsuro Urushidani

(トランスクリプトーム)を網羅的に解析する」毒性学的手法，すなわち「トキシコゲノミクス」である．薬物により非常に低い確率で「予期せぬ」毒性が生じるとしても，その原因となる事象は生体内に必ず生じているはずであり，観測可能なはずである．もしそのすべての事象を観測することができ，その因果関係を解明することができれば，原理的には予測が可能である．生体のすべての生理学的変化を観測する—現実的にはこんなことは不可能であるが，テクノロジーの進歩は，これに近いことを可能にした．マイクロアレイ技術の発達により，1回の実験で実質的に全遺伝子の発現値を定量することが可能となったのである．

2. トキシコゲノミクスプロジェクト

このような背景のもと，厚生労働省，国立医薬品食品衛生研究所(国衛研)，および日本製薬工業協会のワーキンググループは官民共同の「トキシコゲノミクスプロジェクト」(TGP1)を企画した(2)．これは2002年からの5年のプロジェクトであり，以後企業合併などがあって，終了時には，医薬基盤研究所を中核として，国衛研と製薬15社(エーザイ，大塚，小野，キッセイ，三共，三和化学，塩野義，大日本住友，第一，武田，田辺，中外，アステラス，三菱ウェルファーマ，持田)の共同研究体制であった．

TGP1開始当初の計画は以下の通りであった．まず，医薬品を中心とした150の化合物を用い，対象臓器は肝臓を主とすること．これは医薬品の有害作用の多くがこの臓器に絞られること，またそれを構成する細胞種が比較的均一であり，ノウハウを蓄積するには都合がよいためであった．勿論，腎毒性も重要な問題であり，すべての検体について肝臓のみでなく腎臓のサンプリング，病理検査を施行し，一部腎臓の発現解析も実施した．動物はラットを選択した．プロジェクト開始時点ではまだラットの全ゲノム解析は終了しておらず，マウスを用いるべきであるとの意見もあった．しかし，古典的な毒性試験はすべてラットを用いて行われており，膨大なデータの蓄積があった．トキシコゲノミクス手法による毒性予測という，新しい課題に挑戦する場合，この知識を利用しない手はない．また，血液生化学など，遺伝子発現データ以外の情報もマウスより豊富に得られるのも利点であった．

本プロジェクトを計画していた時点で，欧米の大製薬企業やバイオベンチャー企業は既にデータベースの作成を開始しており，出遅れの感は否めなかった(3)．そこで先行するものに対抗できる特長を模索し，表に示すようなプロトコールを採用した．Affymetrix GeneChipを用いることによる定量性・再現性に優れたデータを，多段階の用量・時点で収集し，これに各種の充実した毒性学的データをリンクさせることができた．また，培養細胞を用いた種差のブリッジングも考慮に入れた．

選択された150の化合物(http://wwwtgp.nibio.go.jp/seika.html参照)は，各治療領域を網羅して，肝・腎毒性を示す医薬品の代表的なカテゴリーに属する，いわば「毒性学の教科書」である．これまでに多くのトランスクリプトームデータベースつくられてきたが，これだけの数の医薬品に関して用量や時点のデータがそろっている例はほとんどなく，世界に誇れるものである．

TGP1の5年間で24000匹のラットの犠牲のもとに，8億件以上の遺伝子発現データと，これにひもづけられた288万項目の血液生化学データ，48000件以上の病理組織データが得られ，さらにこれを探索・解析するツール，判別分析などの予測ツールに結果のビューワーを加え，統合データベースシステム：TG-GATEs (Genomic Assisted Toxicity Evaluation System by ToxicoGenomics project)を完成することができた．

オミクス技術の概説，その毒性学への応用と問題点に関しては別稿(4)を参照されたいが，基本的には，遺伝子発現パターンをある特定の毒性に関連づける作業である．それはたとえば最近のデジカメやタスポの顔認識システムに似ている(事実，繁用されるsupport vector machineという判別方式は，TG-GATEsの予測プログラムにも組み込まれている)．ある特定の毒性学的フェノタイプと，複数の遺伝子の発現パターンを抽出して関連付ける．顔認識の場合は，多数の顔の画像を収集して，眼や鼻の位置をコンピューターに学習させ，判別器を作成することになるが，毒性の場合は「どれが眼か鼻かをコンピューターに学習させること」に対応する部分に困難さがある．

表 TGP1のプロトコール

In vivo	
動物	Sprague Dawley rat 6 week old N=5
溶媒	0.5% methylcellulose または corn oil
用量	Low, middle, high (1 : 3 : 10) 経口(一部静脈内，腹腔内)
剖検	単回投与後3，6，9，24時間 連続投与3，7，14，28日後，最終投与後24時間
標本採取・保存	肝臓，腎臓，血漿
GeneChip解析	N=3(肝臓は全化合物，腎臓は30化合物)
検査項目	病理組織：肝臓，腎臓 体重，臓器重量(肝，腎)，摂餌量，血液生化学，血液学(37項目)
In vitro: rat	
動物	Sprague Dawley rat 6 week old
細胞	コラゲナーゼ消化法による肝実質細胞
溶媒	培地またはDMSO(上限0.1%)
濃度	Low, middle, high (1: 5: 25)
処置時間	2，8，24時間
GeneChip解析	Duplicate
検査項目	細胞生存率(LDH遊離，およびDNA量)
In vitro: human	
細胞	ヒト凍結肝細胞
(その他の項目はラットと同様)	

コンピューターは遺伝子の毒性学的意味を知らない（人間の知識が足りないので教え込めない）ので，見かけ上相関のある遺伝子を採用してしまう．これが「遺伝子型」であれば確定した値なので問題は少ないが，「遺伝子発現変動」には生物学的なばらつきが含まれるため，生物学的に無意味で再現性のない判別器が生まれてしまう．この問題は，巨大なデータベースを用いてバリデーションを繰り返せばある程度克服できる．しかしこの戦略には本質的な欠陥がある．

たとえ古典的な毒性学的フェノタイプが遺伝子発現変化と結び付いたとしても，これだけでは何のためにマイクロアレイ実験を行ったのかわからない．そのフェノタイプを測定すればそれで済むのであるから．これに意味があるとすれば，古典的な毒性学手法よりも感度が高いか，早期判定できるかのどちらかのメリットが要求される．医薬品の場合は生体に作用することが前提であり，当然多くの生理応答が期待される．この応答を，治療量で起こるべきものと，不必要な有害反応に切り分けることが必要となるが，現在の知識ではこれは不可能に近い．また後者に関しては，最終的な毒性学的フェノタイプに至る複雑な過程が完全に理解できていないと，特定の遺伝子の初期応答が，将来重大な有害作用につながるか否かを判断することができない．

生体の病態生理学的機構が完全に解明されないと意味のある安全性予測は不可能である，というのはあまりに悲観的な見方である．毒性学者は手をこまねいているわけではない．むしろトキシコゲノミクス手法によって，逆に毒性学的パスウェイを積極的に解明していくということが求められている．

3. 種差の壁

ラットの実験結果を詳細に検討すれば，「ある化合物のラットでの毒性予測」は可能となろうが，それでは不満が残る．医薬品開発ではあくまでもヒトにおける安全性評価が最終目標である．本データベースの直接の目的は，非臨床安全性試験の合理化・加速化であるが，特に外部評価においては，ヒトにおける安全性への寄与を強く要求されるのが常である．最近マイクロドーズ試験が注目されているが，これは主に体内動態を見るものであって，間接的には安全性評価に寄与するかも知れないが，薬理量より遙かに低い量で安全性を判断するのは極めて困難といえよう．ヒトの個体を対象とした直接的な毒性評価が不可能である以上，何らかの代替法を採用せねばならない．

トキシコゲノミクス手法で種差を克服するには，原理的に次のような4つの戦略が考えられる．

1）培養細胞を用いる方法

予備検討において，HepG2のようなライン化された細胞での遺伝子発現変化は正常な肝臓とは大きく異なることが確認され，TGP1ではヒト凍結肝細胞とラット一次培養肝細胞を用いた試験を行うこととした．すなわち，ラットのin vivo→ラットのin vitro→ヒトのin vitro→（ヒトのin vivo）というブリッジングである．

TG-GATEsには，一群の遺伝子における応答性をin vivoとin vitroを並列して一覧する機能，ヒトとラット間のオーソログ変換を自動的に行い，遺伝子リストの種間比較する機能などが装備されている．しかしながらin vitroとin vivoのデータが蓄積されて行くにつれ，解決すべき問題が山積していることを強く認識せざるを得なかった．極端に言えば，ヒト・ラット間の差よりもラットのin vivoとin vitroの差の方が大きいかもしれない．これはヒト由来の細胞を用いたとしてもin vitroからin vivoへの外挿が困難で，培養細胞のデータは非常に限定的な使用に限られてしまうことを意味する．直接の細胞毒性であれば外挿は容易であろうが，臨床における有害作用は，血流や神経を介したものが多く，また，肝障害が生じているような状況下では，非実質細胞（培養系ではほとんど除かれている）の関与が大きいことが知られている．さらに，薬物それ自身ではなく代謝活性化を受けたものが毒性の本体である場合も多いが，培養条件下では生体のような薬物代謝は期待できない．培養法の工夫で改善はされて行くであろうが，現在のところはin vitroで再現可能な毒性学的パスウェイをなるべく多く見いだして，これを参照するという使い方がベストであろう．

2）ヒト型臓器を持った動物を用いる方法

これには主にマウスを利用した2つの方法がある．一つは，ヒト型遺伝子を組み込む方法であり，他方は，ヒトの臓器を移植・定着させる方法である．前者は，すべての関連遺伝子をヒト化することが困難なこと，プロモーター領域込みでヒト化しないとモデルとして成立しないことなどの欠点がある．従って特定の遺伝子の関与を研究する場合にはよいが，一般的なスクリーニングに利用するには程遠い．後者として，免疫不全マウスの肝臓をヒト肝細胞で置き換えたモデルが作られているが(5)，高価であること，免疫不全状態という特殊な環境下での毒性発現が臨床に外挿できるか，など問題が多く，これも一般化は困難である．安全性試験は標準化される必要があり，当分は研究的な使用に限られるであろう．

3）血液サンプルを用いたトランスクリプトーム

ラット肝臓における特定の遺伝子群の発現パターン変化からある医薬候補品の毒性が良好に予測でき，ヒトでの再現が期待されたとしても，臨床治験で患者の肝生検を行うことは非現実的である．非臨床データを臨床につなげるには，非侵襲的サンプルが望まれる．これには，非臨床での遺伝子発現データから予測される血中あるいは尿中の代替マーカーを提案するか，あ

るいは生検しなくても得られるサンプルの遺伝子発現を測定するしかない．前者の場合，薬物の毒性発現に相関して発現変化する遺伝子があったとしても，その遺伝子産物が細胞外に出てこない限り検出できない．遺伝子産物が分泌されるものであれば，血中に反映されるのは，発現に対する効果と分泌に対する効果を合わせた結果でしかない．非分泌型のものであれば，血中で検出されるということは細胞の破壊を意味し，古典的な逸脱酵素の検出と変わらないことになる．ただし，逸脱酵素より遙かに感度と特異性が高ければ，臓器特異的 mRNA の漏出を測定する意味はある(6)．

後者の候補としては，血液中の白血球がほとんど唯一のものである．薬物投与時に全身で起こる有害作用が，直接あるいは間接的に白血球の遺伝子発現変化として反映されることを期待している．実際，ラットにおいて，アセトアミノフェン投与により薬物特異的な遺伝子変化が検出できたとの報告があり(7)，また，臨床研究も進められている．

4）毒性学的パスウェイを介したブリッジング

これまでの経験では，動物細胞において薬物の毒性に特徴的な遺伝子群の変化が認められたとしても，これらを単純にオルソログ変換したものは，ヒト細胞における発現変化を示す遺伝子群と低い一致率しか示さない．しかし，個々の遺伝子同士の対応は低いにしても，毒性物質に対する「機能遺伝子群」としての病理的応答は共通性が見いだせる場合がある．そこで，動物実験で得られた結果を，毒性学的パスウェイ上にマッピングして「ヒトにおいてもこのようなメカニズムで毒性が発現する危険がある」ことを提示することは，合理的な手法と考えられる．これは前述した「毒性学的パスウェイ」解明の重要性を示すものであり，現在最も期待すべき戦略といえよう．

4. トキシコゲノミクス・インフォマティクスプロジェクト（TGP2）

トキシコゲノミクスが各国で走り出した頃は，データベースさえ構築すれば，あとはコンピューターを駆使して何とかなるだろう，という考えがあったように思う．特に 2005 年，FDA が新薬の申請時にゲノミクスデータのボランタリーサブミッションを開始したことから，この分野に注目が集まった．しかしながら，データが集積するにつれ，それは余りに楽観的であることが明らかになってきた．最近の FDA をはじめとする世界的な動向では，ゲノミクスデータを安全性試験に応用するには，バイオマーカーという形で提示することが求められる方向にある(8)．バイオマーカーは FDA の定義によれば「生物学的プロセスや病理学的プロセス，あるいは治療に対する薬理学的な反応の指標として客観的に測定・評価される項目」であり，トキシコゲノミクスであれば，遺伝子（群）の発現パターンと判定アルゴリズムのセットであり，特定の毒性学的フェノタイプの診断・予測，あるいは毒性メカニズムの評価ができるものと定義される．そして，安全性試験に資するものであるためには，再現性を保証するバリデーションが必須である．このようなバイオマーカーの取得には，前述のように，多くの課題があるため，TGP1 の後継プロジェクトとして，トキシコゲノミクス・インフォマティクスプロジェクト（TGP2）が組織された．TGP1 と同様に，医薬基盤研を中核として，国衛研，製薬 13 社（アステラス，エーザイ，大塚，小野，キッセイ，三和化学，塩野義，住友化学，第一三共，大日本住友，武田，田辺三菱，中外）が参画する官民共同プロジェクトである．TGP2 の目的は，TG - GATEs を活用し，多くの安全性バイオマーカーを創出すること，前述の血液のトランスクリプトミクスに加えメタボロミクスなど他のテクノロジーをも含めた多彩な戦略により種差のブリッジングを果たすこと，そして，これらの成果を創薬につなげるため，トキシコゲノミクスをレギュラトリーサイエンスに利用する基盤を築くこと，の 3 点に集約される．現在はまだ TGP2 が進行中であるが，成果の一部については，最近の総説(9) を参照されたい．

おわりに

トキシコゲノミクスをはじめとするオミクステクノロジーは，すべての現象を把握しなければならない毒性学者にとって，必須の技術である．タンパク質や代謝物の変化も当然重要であり，プロテオミクスやメタボロミクスを加えて統合した，トキシコパノミクスという概念すら導入されるに至っている．ただしこれらを創薬に結びつけるには再現性の保証された安全性バイオマーカーという形に仕上げる必要があり，これは現在のプロジェクトの重要な使命である．また，ヒトにおける安全性研究も，更なる飛躍が望まれる．その一つの試みとして，iPS 細胞を各臓器の細胞に分化させ，トランスクリプトミクスと結びつけることによって，ヒトの遺伝子型別の安全性試験系の構築を目指した研究が，医薬基盤研を中心に始められている．

文　献

1) Kola I, et al. Nature Rev Drug Discov. 2004;3:711-715.
2) Urushidani T. Hepatotoxicity. Wiley; 2007. p. 507-529.
3) Boverhof DR, et al. Toxicol Sci. 2006;89:352-360.
4) 漆谷徹郎. 日薬理誌. 2009;133:112-114.
5) Ohashi K, et al. Nature Med. 2000;6:327-331.
6) Kudo Y, et al. Vet Med Sci. 2008;70:993-996.
7) Bushel PR, et al. Proc Natl Acad Sci U S A. 2007;104:18211-18216.
8) http://www.fda.gov/oc/initiatives/criticalpath/
9) Uehara T, et al. Mol Nutr Food Res. 2009;54:218-227.

NANOS2 interacts with the CCR4-NOT deadenylation complex and leads to suppression of specific RNAs

Atsushi Suzuki[a], Katsuhide Igarashi[b], Ken-ichi Aisaki[b], Jun Kanno[b], and Yumiko Saga[c,1]

[a]Interdisciplinary Research Center, Yokohama National University, Yokohama, Kanagawa 240-8501, Japan; [b]Cellular and Molecular Toxicology Division, National Institute of Health Sciences, Setagayaku, Tokyo 158-8501, Japan; and [c]Division of Mammalian Development, National Institute of Genetics, Mishima 411-8540, Japan

Edited by Ruth Lehmann, New York University Medical Center, New York, NY, and approved December 30, 2009 (received for review August 2, 2009)

Nanos is one of the evolutionarily conserved proteins implicated in germ cell development. We have previously shown that NANOS2 plays an important role in both the maintenance and sexual development of germ cells. However, the molecular mechanisms underlying these events have remained elusive. In our present study, we found that NANOS2 localizes to the P-bodies, known centers of RNA degradation that are abundantly accumulated in male gonocytes. We further identified by immunoprecipitation that the components of the CCR4-NOT deadenylation complex are NANOS2-interacting proteins and found that NANOS2 promotes the localization of CNOT proteins to P-bodies in vivo. We also elucidated that the NANOS2/CCR4-NOT complex has deadenylase activity in vitro, and that some of the RNAs implicated in meiosis interact with NANOS2 and are accumulated in its absence. Our current data thus indicate that the expression of these RNA molecules is normally suppressed via a NANOS2-mediated mechanism. We propose from our current findings that NANOS2-interacting RNAs may be recruited to P-bodies and degraded by the enzymes contained therein through NANOS2-mediated deadenylation.

germ cells | P-body | meiosis

In the mouse, the primordial germ cells (PGCs) are segregated from the somatic cell lineage at an early gastrulation stage (1). Although the PGCs are potent producers of both oogonia and spermatogonia, sexual differentiation is induced after their colonization of the embryonic gonads with somatic cells. However, the initial steps leading to diversification of these cells have long remained unsolved. Retinoic acid (RA) signaling has recently been identified as the initial trigger for feminization (2). RA molecules derived from the mesonephros trigger meiotic initiation in female gonocytes via the induction of the RA responsive gene *Stra8*, which is required for premeiotic replication (3). In contrast, male gonocytes are protected from exposure to RA by CYP26B1, an RA metabolizing enzyme produced from somatic cells, resulting in the suppression of meiosis up to E13.5 (4, 5). In addition, *Nanos2* expression begins after E13.5 and is required for the maintenance and promotion of the male germ cell state (6).

Nanos is an evolutionarily conserved RNA-binding protein that is essential for germ cell development (7). In *Drosophila*, Nanos forms a complex with another RNA-binding protein, Pumilio, and represses the translation of the *hunchback*, *cyclin B*, and *hid* mRNAs thereby establishing embryonic polarity, mitotic quiescence, and suppression of apoptosis, respectively (8–10). Three *Nanos* homologs, *Nanos1–3*, exist in the mouse, among which *Nanos3* and *Nanos2* are expressed in the germ cells and are required to protect these cells from undergoing apoptosis during migration and after colonization of the male gonads, respectively (11, 12). In addition, *Nanos2* plays a key role during the sexual development of germ cells by suppressing meiosis and promoting male-type differentiation in the embryonic male gonads. Moreover, the forced expression of *Nanos2* in female gonocytes can induce the suppression of meiosis and promotion of male-type gene expression (6). However, the molecular mechanisms underlying how this protein accomplishes such pleiotropic functions in the mouse germ cells remain unknown.

In our present study, we find that NANOS2 localizes to P-bodies, a central hub of RNA degradation (13, 14). We further identify components of the CCR4-NOT deadenylation complex as NANO$2-associated proteins in vivo, which can cleave poly(A) RNA in vitro. We also show that specific mRNAs interact with NANOS2, and thus propose that NANOS2 plays a role in recruiting the CCR4-NOT deadenylation complex to trigger the degradation of specific RNAs.

Results

NANOS2 Localizes at P-Bodies During Gonocyte Development. To increase our understanding of the molecular mechanisms underlying the function of the NANOS2 protein, we first analyzed the cellular localization of this protein by immunostaining. Consistent with the results of our previous western analyses (15), NANOS2 protein was first detectable at E13.5 in the cytoplasm of male mouse gonocytes. This signal intensity increased until about E16.5 and then slightly decreased by E17.5. In addition, we found that some of the NANOS2 proteins formed discrete foci, the number of which gradually increased until E16.5 and then decreased thereafter (Fig. S1 *A–F*). Because *Drosophila* Vasa and Tudor are known to form cytoplasmic foci (16, 17), which are the polar granules in the germ plasm, we speculated that these NANOS2 foci might colocalize with the mouse homologs of Vasa, MVH (mouse vasa homolog) (18) and the Tudor protein TDRD1 (tudor domain containing 1) (19). However, these foci did not show any clear colocalization with NANOS2 (Fig. S2 *A–F*). We next tested the possibility that the NANOS2 foci might correspond to P-bodies, which are known to function as a center of RNA degradation. We thus conducted double-immunostaining using antibodies against the P-body components DCP2 and XRN1, an mRNA decapping enzyme and RNA exonuclease, respectively (13, 14). We were initially surprised to find that many P-bodies could be specifically observed only in germ cells and not in the somatic cells in E15.5 male gonads, and also that the NANOS2 foci clearly merged with those of DCP2 and XRN1 (Fig. 1 *A–F*) from E13.5 to E17.5 (Fig. S3 *A–F*). This suggests the possibility that NANOS2 may be involved in RNA degradation.

Nanos2 Functions in the Formation of P-Bodies. We further examined the status of the P-bodies in the mouse gonads of both sexes by immunostaining of p54/RCK, a homolog of *Drosophila* Me31B and also a marker of these structures (20). Although the P-bodies seemed to be present in the same number and size in the gonocytes of both sexes at E12.5, they were gradually reduced and eventually lost by E14.5 in female gonocytes (Fig. S4 *E* and *F*). In contrast, the P-bodies become much larger in both number and

Author contributions: A.S. and Y.S. designed research; A.S., performed research; K.I., K.. A., and J.K. analyzed data of microarray analyses; and A.S. and Y.S. wrote the paper.

The authors declare no conflict of interest.

This article is a PNAS Direct Submission.

[1]To whom correspondence should be addressed. E-mail: ysaga@lab.nig.ac.jp.

This article contains supporting information online at www.pnas.org/cgi/content/full/0908664107/DCSupplemental.

www.pnas.org/cgi/doi/10.1073/pnas.0908664107

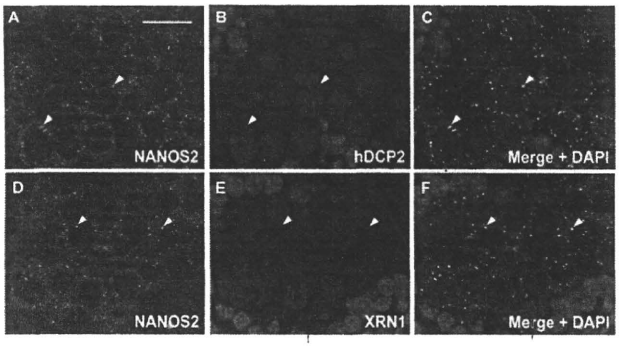

Fig. 1. NANOS2 localizes to the P-bodies in male mouse gonocytes. (*A–L*) Sections prepared from wild-type E15.5 male gonads were double-stained with mouse anti-NANOS2 (green) (*A* and *D*) and either hDCP2 (*B*) or mXRN1 (*E*) antibodies (red staining in each case). Arrowheads indicate colocalization of NANOS2 and hDCP2 (*C*) or XRN1 (*F*). DNA was counterstained with DAPI (blue). (Scale bar in *A*, 20 μm for all panels.)

size from E14.5, concomitant with the onset of NANOS2 expression, in male gonocytes (Fig. S4 *A–D*).

To further explore the role of NANOS2 in P-body formation, we examined the status of these structures in the absence of *Nanos2*. Although there were, somewhat unexpectedly, many P-bodies detected in both *Nanos2*$^{+/-}$ and *Nanos2*$^{-/-}$ male gonocytes at E13.5, their sizes became gradually larger, whereas their number became smaller, at the later stages of embryogenesis in the absence of *Nanos2* (Fig. 2 *A–D*). This was also observed in *Nanos2, Bax* double-null male gonocytes (Fig. 2 *E* and *F*), where apoptotic cell death was suppressed, suggesting that apoptosis does not affect P-body status. This indicates that NANOS2 is not essential for the assembly of P-bodies but is required for the maintenance of their normal state. To further elucidate the functions of NANOS2 in P-body formation, we also examined the status of the P-bodies in NANOS2-expressing female gonocytes (6). Although they could not be detected in normal female gonocytes at E16.5, we found many P-bodies in NANOS2-expressing female cells and additionally observed that NANOS2 localizes at the P-bodies in these cells (Fig. 2 *G–I*). These data indicate that NANOS2 is sufficient to maintain the number of P-bodies when female gonocytes have acquired a male-type phenotype due to NANOS2 expression.

NANOS2 Interacts with the CCR4-NOT Deadenylation Complex and Regulates Its Localization. To explore the molecular functions of NANOS2, we searched for proteins that interact with it. To this end, we prepared male gonadal extracts from *Nanos2*$^{+/-}$ and *Nanos2*$^{-/-}$ embryos at E14.5 and subjected them to immunoprecipitation with anti-NANOS2 antibodies. We found that two major bands of more than 200 kDa were exclusively precipitated from *Nanos2*$^{+/-}$ gonads, and by mass spectrometric analysis identified these products as CNOT1, a component of the CCR4-NOT deadenylation complex (13) (Fig. 3A).

In further immunoprecipitation experiments, we used a transgenic mouse line expressing a FLAG-tagged NANOS2 under the direct control of the *Nanos2* enhancer (15) (Fig. S5*A*), since we had confirmed that this fusion protein was functional (Fig. S5 *B–F*) and localized at the P-bodies (Fig. S5 *G–I*). Western analyses revealed that CNOT1 coprecipitates with FLAG-tagged NANOS2 (Fig. 3*B, Upper*), confirming the results of our mass spectrometric analysis. We also found that other components of the CCR4-NOT complex, CNOT3, CNOT6L/Ccr4b, CNOT7/Caf1a, and CNOT9/Rcd1 (13, 21), also coprecipitated with FLAG-tagged NANOS2, indicating that NANOS2 associates with the CCR4-NOT deadenylation complex in vivo. We additionally found that this interaction is independent of RNA, as the levels of coprecipitated CNOT proteins were not affected by treatments with RNase (Fig. 3*B*). Finally, these CNOT proteins were found to colocalize with NANOS2 in P-bodies (Fig. 3 *C–E* and Fig. S6 *A–I*), suggesting that this complex may play a role in the activities of these elements.

To better understand the physiological significance of its interaction with NANOS2, we investigated the localization of CCR4-NOT deadenylation complex in *Nanos2*$^{-/-}$ male gonads by immunostaining CNOT proteins with DCP1A, another decapping enzyme and also a component of P-bodies (13, 14). Although CNOT3 was found to clearly localize to P-bodies in *Nanos2*$^{+/-}$ male gonads (Fig. 3 *F–H*), we detected only weak signals for this protein in P-bodies in the absence of NANOS2 (Fig. 3 *I–K*) even though the levels of CNOT3 are not reduced in *Nanos2*$^{-/-}$ male gonads (Fig. 3*L*). We obtained similar results for CNOT1 (Fig. S7). These data suggest that NANOS2 promotes the localization of the CCR4-NOT deadenylation complex to P-bodies, although a subpopulation of this complex still remains in these structures in the absence of NANOS2, possibly via a NANOS2-independent mechanism. Based on these findings and the fact that the CCR4-NOT deadenylation complex regulates the first step of mRNA degradation (22), we speculate that NANOS2 recruits this deadenylation complex to P-bodies where it promotes the degradation of RNAs.

Complex of NANOS2 and CCR4-NOT Deadenylase Complex in Male Germ Cells Retains Deadenylase Activity. To address the critical question of whether NANOS2-interacting deadenylase actually has catalytic activity, we used NANOS2-overexpressing (NANOS2 O/E) adult testes to obtain sufficient amounts of this protein and thus overcome the limitations of using embryonic testis in biochemical analyses. In the testis of the postnatal mouse, NANOS2 is expressed in a small population of undifferentiated spermatogonia (23) and localizes to P-bodies (Fig. S8 *A–C*) as in the male gonocytes. This expression is subsequently lost as these cells differentiate. However, if FLAG-tagged NANOS2 is forcedly and continuously expressed in the spermatogonial population, the male mouse become infertile because the spermatogonia remain in an undifferentiated state in the testis, in which a large number of NANOS2-positive spermatogonia occupy the periphery of the seminiferous tubules (23). In addition, FLAG-tagged NANOS2 also localizes to the P-bodies in the spermatogonia in the manner similar to endogenous Nanos2 (Fig. S8 *D–F*). We prepared testis extracts from this mouse and performed immunoprecipitations with anti-FLAG antibodies and control IgG, and then subjected these immunoprecipitates to in vitro deadenylase assay (21) (Fig. 4*A*). As shown in Fig. 4*B*, cleavage of the poly(A) RNA substrate occurred only with NANOS2 immunoprecipitates, which also contains the CNOT6L and CNOT7 catalytic components of the deadenylation complex (Fig. 4*C*). These results lead us to propose that NANOS2 promotes the degradation of NANOS2-interacting mRNAs through the deadenylase activity of the CCR4-NOT complex.

NANOS2 Interacts with Specific mRNAs and May Promote Their Degradation. Based on our working hypothesis, we further speculated that (*i*) the NANOS2 complex should contain specific mRNAs that would be degraded via NANOS2-mediated deadenylation, such that (*ii*) the expression levels of these transcripts would be low in wild-type male gonocytes but up-regulated in the absence of NANOS2. To test these possibilities, RNAs that coprecipitated with FLAG-tagged NANOS2 were purified and subjected to RT-PCR. Because we had previously shown that male gonocytes could enter meiosis in the absence of NANOS2, it was plausible that mRNAs involved in meiosis might be directly suppressed through NANOS2-mediated RNA degradation. As expected, *Sycp3*, *Stra8*, *Taf7l*, *Dazl*, and *Meisetz* (3, 24–27) transcripts that are implicated in meiosis were specifically detected only in the NANOS2 protein precipitates despite their very low expression in male gonads (Fig. 5 *A* and *B*). In contrast, the

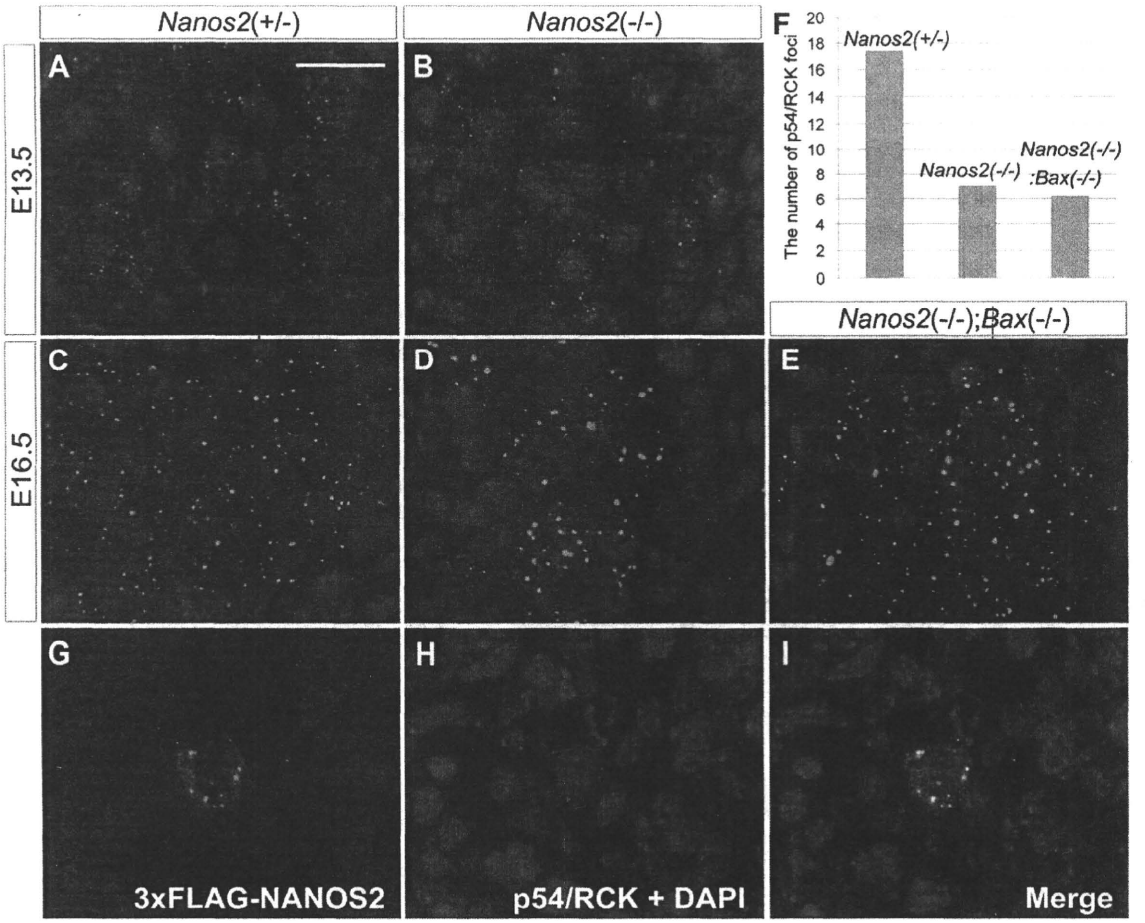

Fig. 2. Functional role of NANOS2 during the formation of the P-bodies. (*A–E*) Male gonadal sections from *Nanos2*$^{+/-}$ (*A* and *C*), *Nanos2*$^{-/-}$ (*B* and *D*), and *Nanos2*$^{-/-}$*Bax*$^{-/-}$ (*E*) embryos at stages E13.5 (*A* and *B*), and E16.5 (*C, D,* and *E*) were immunostained with p54/RCK (green) and TRA98 (red) antibodies. (*F*) Average number of p54/RCK foci per male gonocyte at E16.5 was quantified in each picture using ImageJ software (National Institutes of Health) and a cell counter, with the foci of less than a 20 permission value excluded using Photoshop (Adobe). The data shown correspond to two to three pictures. (*G–I*) A female gonadal section from a NANOS2-expressing embryo at E16.5 was immunostained with anti-FLAG (green) (*G*) and anti-p54/RCK (red) (*H*) antibodies. DNA was counterstained using DAPI (blue). (Scale bar in *A,* 20μm for *A–E* and *G–I.*)

G3pdh, *Dnmt3l* and *Dnmt3a* mRNAs did not show specific accumulation in the NANOS2 precipitates although they are all highly expressed in male gonads. These data indicate that the mRNAs involved in meiosis specifically interact with NANOS2 in vivo.

We next investigated global changes in gene expression upon the loss of *Nanos2* using comparative GeneChip analyses (Table S1). The resulting scatter plots showed that many genes become up- or down-regulated in *Nanos2*$^{-/-}$ male gonads by E15.5 (Fig. S9 *A–C*). For example, we found that the genes highly expressed only in male gonocytes, such as *Dnmt3l*, *Tdrd1* and *Miwi2*/*Piwi-like 4* (19, 28, 29), are down-regulated in the *Nanos2*$^{-/-}$ male gonads, whereas *Figla*, *Lhx8* and *Nobox*, which have been shown to be essential only for oogenesis and not for spermatogenesis (30–32), become accumulated in the *Nanos2*$^{-/-}$ male gonads (6) (Fig. S9 *D–I*). These results suggest that male gonocytes cannot enter the male pathways and become feminized by the up-regulation of female-type genes. In addition, and consistent with the results of our immunoprecipitation assay, *Sycp3*, *Stra8*, *Taf7l*, *Dazl,* and *Meisetzs* mRNAs were also found to be up-regulated in *Nanos2*$^{-/-}$ male gonads (Fig. 5 *C–G*). Our current findings thus indicate that NANOS2-interacting mRNAs become accumulated if NANOS2 is absent in male gonocytes, which in turn indicates that NANOS2 might be indirectly affecting the transcription of these genes, or that they are normally suppressed in wild-type male gonocytes through a NANOS2-directed mechanism, possibly a deadenylation pathway.

Discussion

Molecular Role of NANOS2. In our current study, we show that the CCR4-NOT deadenylation complex is coprecipitated with NANOS2 from male gonadal extracts. This is the first evidence that the interaction between a Nanos homolog and the CCR4-NOT deadenylation complex exists *in vivo,* although it has been shown using a yeast two-hybrid system that *Drosophila* Nanos can directly and potently bind to NOT4, a component of the CCR4-NOT complex (33). Hence, as suggested previously by Kadyrova et al. for *Drosophila* Nanos, and as confirmed by our present analyses in vivo, the recruitment of the CCR4-NOT deadenylation complex to target mRNAs may be a conserved function of the Nanos proteins.

We also found that NANOS2 localizes to P-bodies in the male gonocytes and adult mouse spermatogonia. P-bodies are known to be a central hub of RNA degradation, in which decapping enzymes and exonucleases are also localized. However, emerging evidence in other systems suggests that P-bodies not only function to degrade RNAs but also to store mRNAs in a translationally quiescent state until needed (13). In addition, *Drosophila* Nanos promotes the deadenylation of poly(A) tail in *hunchback* mRNA and represses its translation without changing the mRNA level

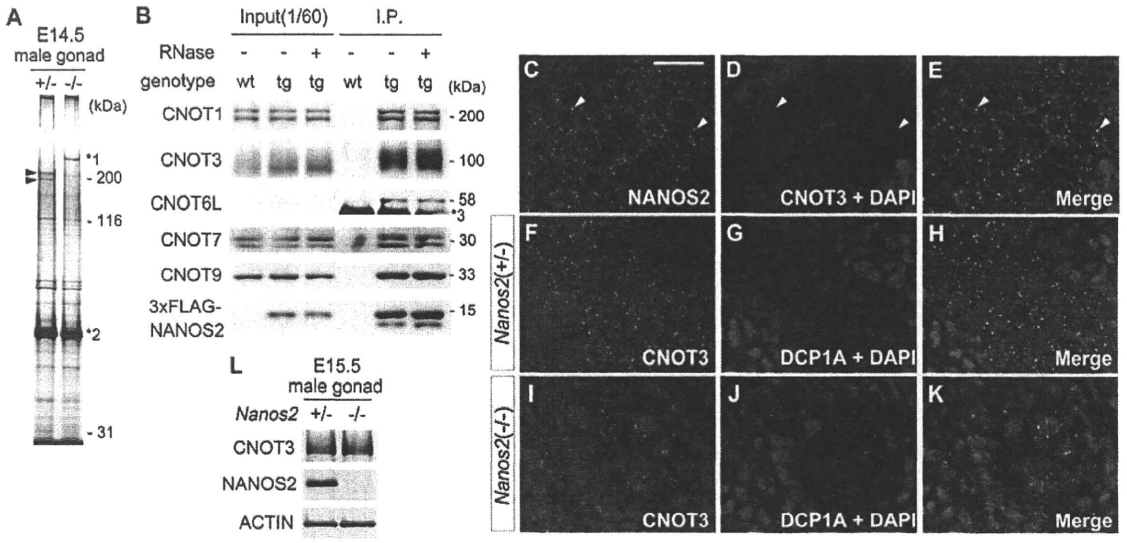

Fig. 3. Interaction between NANOS2 and the CCR4-NOT deadenylation complex. (*A*) Proteins coimmunoprecipitated with NANOS2 from E14.5 wild-type (lane 1) and *Nanos2*$^{-/-}$ (lane 2) male gonadal extracts using rabbit anti-NANOS2 antibodies. Arrowheads indicate CNOT1. *1, nonspecific band; *2, IgG polypeptide. (*B*) Immunoprecipitation–Western blot analyses of proteins from male gonadal extracts of wild-type and transgenic embryos expressing 3×FLAG-NANOS2. *3, IgG polypeptide from the anti-FLAG antibody. (*C–E*) Male gonadal sections from E15.5 embryos were immunostained with mouse NANOS2 (green) (*C*) and CNOT3 (red) (*D*) antibodies. Arrowheads in *C–E* indicate colocalization between NANOS2 and CNOT3. (*F–K*) Male gonadal sections from *Nanos2*$^{+/-}$ (*F–H*) and *Nanos2*$^{-/-}$ (*I–K*) embryos at E15.5 were immunostained with DCP1A (red) (*G* and *J*) and CNOT3 (green) (*F* and *I*) antibodies. DNA was labeled via DAPI counterstaining (blue). (*L*) Western blot analyses of proteins from the male gonads of *Nanos2*$^{+/-}$ and *Nanos2*$^{-/-}$ embryos at E15.5.

(34). We cannot therefore rule out the possibility that NANOS2 not only promotes the degradation of mRNAs involved in meiosis but also retains other transcripts at P-bodies to sequester them in a translationally inactive state during embryogenesis. These transcripts may be released from the P-bodies and translated to promote differentiation after birth as NANOS2 expression begins to disappear.

P-Body Formation in Male Mouse Gonocytes. P-bodies have been well characterized in yeast and mammalian cultured cells, and the in vivo status of these foci has begun to be described recently also in worms and flies (35–38). We found from our current analyses that P-bodies are specifically formed and/or maintained in the germ cells of male mouse embryonic gonads, whereas no such structures are detectable in somatic cells. Furthermore, female mouse gonocytes fail to maintain P-bodies at later stages of embryogenesis. We thus suggest that P-bodies play roles in cell-type specific differentiation during mouse development through RNA metabolism.

It has also been shown that P-bodies are dynamic structures and that their size and number reflects the status of the mRNA supply. If the transit of mRNAs into the P-bodies is inefficient, the size and number of these structures becomes extremely small. In contrast, they become larger when the mRNA decapping pathway is blocked (39, 40). Furthermore, it has been recently reported that deadenylation is required for P-body formation (41). Taking into account the data presented in these earlier reports and our current model, P-bodies would be expected to be small in *Nanos2*$^{-/-}$ male gonocytes because the mRNA supply to these structures and subsequent deadenylation efficiency would be inhibited in the absence of NANOS2. However, we were surprised to find that the sizes of the P-bodies

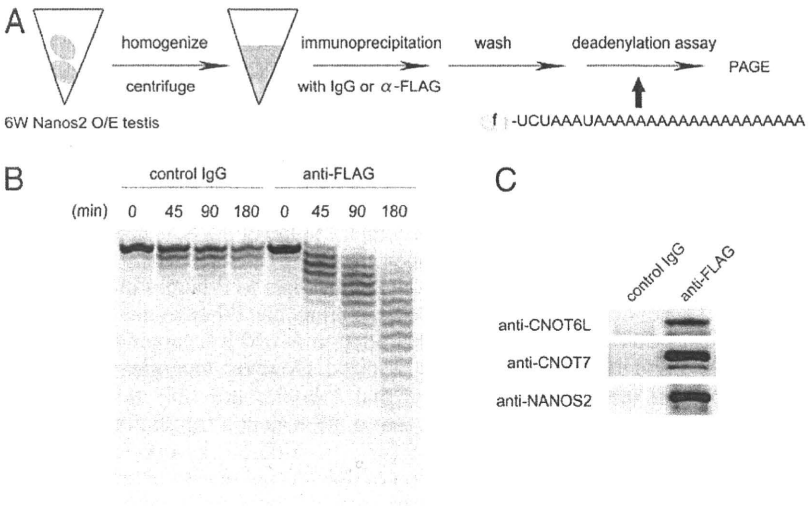

Fig. 4. The protein complex of NANOS2 and CCR4-NOT complex has in vitro deadenylase activity. (*A*) Schematic representation of the in vitro deadenylase assay method using NANOS2 over-expressing (O/E) testes. (*B*) FLAG-tagged NANOS2 was precipitated with anti-FLAG antibodies from the testis extracts of a 6-week-old NANOS2 O/E mouse and incubated with 5′-fluorescein isothiocyanate-labeled poly (A) RNA substrate for 0, 45, 90, and 180 min. Samples were then analyzed on a denaturing sequencing gel, as previously described (**21**) (*G*). (*C*) Western blot analyses reveaing that CNOT6L and CNOT7 are coprecipitated with FLAG-tagged NANOS2.

DEVELOPMENTAL BIOLOGY

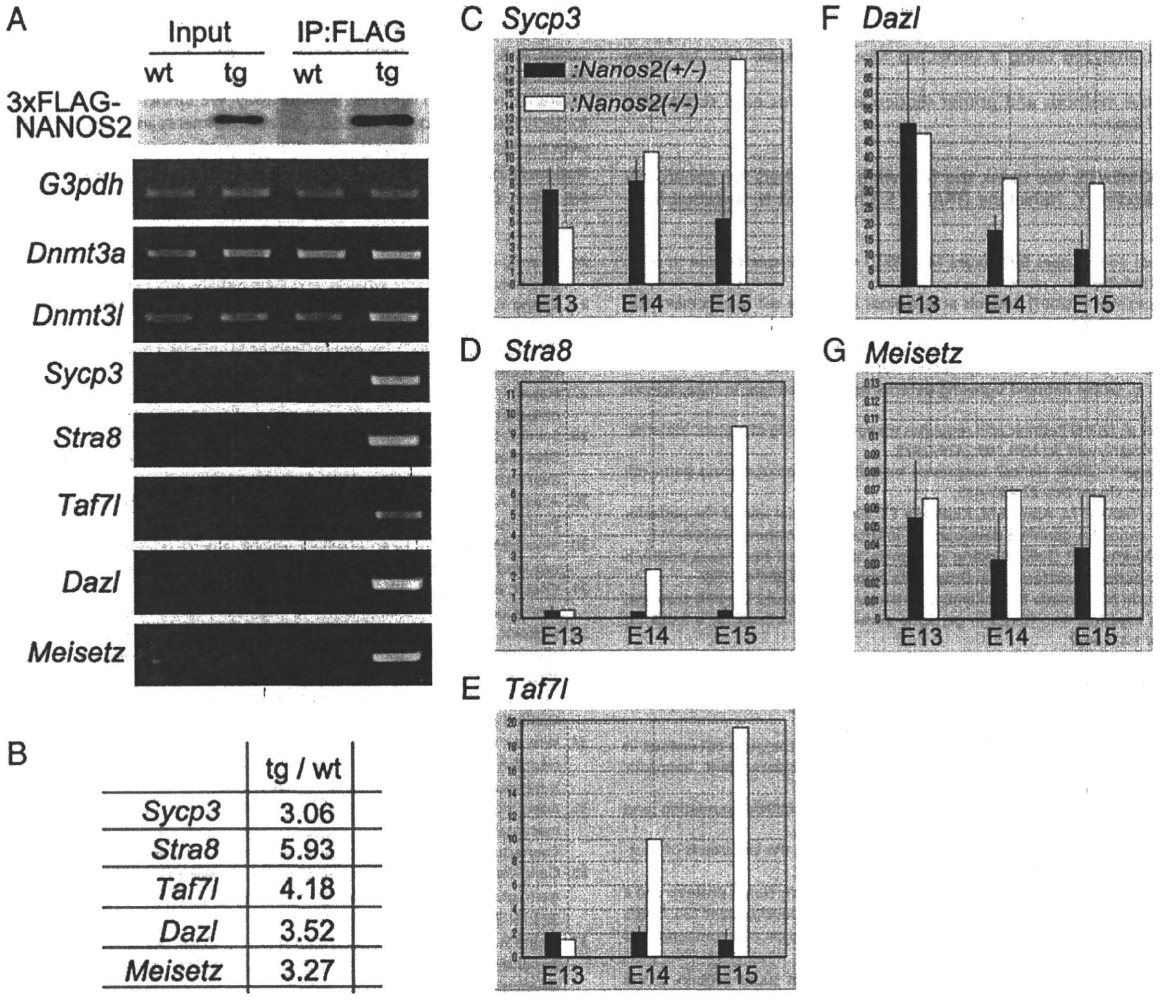

B

	tg / wt
Sycp3	3.06
Stra8	5.93
Taf7l	4.18
Dazl	3.52
Meisetz	3.27

Fig. 5. NANOS2 interacts with specific mRNAs and may promote their degradation. (*A*) Male gonadal extracts from wild-type (*wt*) and transgenic (*tg*) mice expressing FLAG-NANOS2 at E15.5 were subjected to immunoprecipitation (IP) with FLAG antibodies. RNA precipitates were analyzed by semi-quantitative RT-PCR. (*B*) Quantification of each mRNA enrichment from a FLAG IP of *tg* extracts using real-time RT-PCR. Fold enrichment of each mRNA coprecipitated from *tg* compared with those from *wt* is indicated. Mean value of three independent QRT-PCR results is shown. (*C–G*) Expression profiling of the *Sycp3* (*C*), *Stra8* (*D*), *Taf7l* (*E*), *Dazl* (*F*), and *Meisetz* (*G*) genes in male gonads from *Nanos2*$^{+/-}$ and *Nanos2*$^{-/-}$ embryos at E13.5-E15.5 using the Affymetrix GeneChip System as previously described (43) (*X*-axis; embryonic stage, *Y*-axis; expression level, black bars; *Nanos2*$^{+/-}$ embryos, white bars; *Nanos2*$^{-/-}$ embryos).

became larger in this biological context, although their number was decreased. These data thus indicate that male gonocytes have a unique program for P-body formation that occurs both in a NANOS2-dependent and -independent manner.

mRNAs Targeted by NANOS2. We elucidated that the protein complex of NANOS2 and CCR4-NOT complex has deadenylase activity in vitro. We thus expected that the poly(A) tail lengths of NANOS2-interacting mRNAs would be maintained without NANOS2. To test this scenario, we assayed the poly(A) tail length of NANOS2-interacting mRNAs. However, we could not observe clear shortening of the poly(A) tail in wild-type male gonads, possibly because of their low abundance. New experimental systems will be required in the future to address this issue.

On the other hand, it was noteworthy that we identified *Stra8* as a NANOS2-interacting mRNA because we have shown previously that *Stra8* is up-regulated at the transcriptional level in *Nanos2*$^{-/-}$ male gonocytes (6). These data together indicate that the suppression of *Stra8* in male gonocytes is ensured at both the transcriptional and translational levels, suggesting the critical functional importance of suppressing this gene during male gonocyte development.

Materials and Methods

Mice. Both the *Nanos2* and *Bax*-knockout mouse lines and PCR methods used for the verification of each mutant allele have been previously described (11, 42). The NANOS2-expressing mouse line has also been described (23) The transgene containing 3×FLAG-tagged *Nanos2* with the 3′-UTR under the control of Nanos2 enhancer (9.2 kb upstream sequence) was used for the production of the transgenic mouse line.

Histological Methods. For immunostaining, mouse gonads of both sexes were directly embedded in O.C.T. compound (Sakura) and frozen in liquid nitrogen. After sectioning (8 μm), samples were stained according to standard procedures.

Immunoprecipitation. Extracts of male gonads from E14.5 or E15.5 embryos were incubated with protein-A beads crosslinked with rabbit anti-NANOS2 antibody or anti-FLAG M2 affinity gel (Sigma).

In Vitro Deadenylase Assay. The testis extracts from NANOS2-expressing mice were incubated with anti-FLAG M2 affinity gel or Mouse IgG-agarose (Sigma). After several washes, precipitates were then subjected to a deadenylase assay as previously described (21).

RT-PCR. After synthesis of first-strand cDNAs with SuperScript III reverse transcriptase and $(dT)_{20}$ primer (Invitrogen), PCR analyses were carried out either using a regular or real-time protocol.

GeneChip Analysis. Total RNAs were purified from cells corresponding to the male gonads of *Nanos2-LacZ* knock-in heterozygous and homozygous embryos, and analyzed using a GeneChip Mouse Genome 430 2.0 Array (Affymetrix).

Details of the methods and primer sequences used for each section are provided in *SI Text*.

ACKNOWLEDGMENTS. We thank the following researchers for generously providing antibodies: Y. Nishimune (TRA98), S. Chuma and N. Nakatsuji (anti-TDRD1), T. Noce (anti-MVH), M. Kiledjian (anti-hDCP2), W. D. Heyer (anti-mXRN1), H. T. Timmers (anti-CNOT1), T. Tamura (anti-CNOT3), T. Yamamoto (anti-CNOT6L/Ccr4b), A. B. Shyu (anti-CNOT7/Caf1a), and H. Okayama (anti-CNOT9/Rcd1). We are also very grateful to M. Morita and T. Yamamoto for their technical advice and assistance with the *in vitro* deadenylase assay. We further thank Noriko Moriyama for technical assistance with the microarray experiments and Yuki Nakajima for help with the histological analyses. This work was partly supported by Grants-in-Aid for National BioResource Project and of the Genome Network Project of the Ministry of Education, Culture, Sports, Science and Technology, Japan.

1. Hayashi K, de Sousa Lopes SM, Surani MA (2007) Germ cell specification in mice. *Science* 316:394–396.
2. Bowles J, Koopman P (2007) Retinoic acid, meiosis and germ cell fate in mammals. *Development* 134:3401–3411.
3. Baltus AE, et al. (2006) In germ cells of mouse embryonic ovaries, the decision to enter meiosis precedes premeiotic DNA replication. *Nat Genet* 38:1430–1434.
4. Bowles J, et al. (2006) Retinoid signaling determines germ cell fate in mice. *Science* 312:596–600.
5. Koubova J, et al. (2006) Retinoic acid regulates sex-specific timing of meiotic initiation in mice. *Proc Natl Acad Sci USA* 103:2474–2479.
6. Suzuki A, Saga Y (2008) Nanos2 suppresses meiosis and promotes male germ cell differentiation. *Genes Dev* 22:430–435.
7. Kobayashi S, Yamada M, Asaoka M, Kitamura T (1996) Essential role of the posterior morphogen nanos for germline development in Drosophila. *Nature* 380:708–711.
8. Murata Y, Wharton RP (1995) Binding of pumilio to maternal hunchback mRNA is required for posterior patterning in Drosophila embryos. *Cell* 80:747–756.
9. Asaoka-Taguchi M, Yamada M, Nakamura A, Hanyu K, Kobayashi S (1999) Maternal Pumilio acts together with Nanos in germline development in Drosophila embryos. *Nat Cell Biol* 1:431–437.
10. Sato K, et al. (2007) Maternal Nanos represses hid/skl-dependent apoptosis to maintain the germ line in Drosophila embryos. *Proc Natl Acad Sci USA* 104:7455–7460.
11. Tsuda M, et al. (2003) Conserved role of nanos proteins in germ cell development. *Science* 301:1239–1241.
12. Suzuki H, Tsuda M, Kiso M, Saga Y (2008) Nanos3 maintains the germ cell lineage in the mouse by suppressing both Bax-dependent and -independent apoptotic pathways. *Dev Biol* 318:133–142.
13. Parker R, Sheth U (2007) P bodies and the control of mRNA translation and degradation. *Mol Cell* 25:635–646.
14. Eulalio A, Behm-Ansmant I, Izaurralde E (2007) P bodies: At the crossroads of post-transcriptional pathways. *Nat Rev Mol Cell Biol* 8:9–22.
15. Suzuki A, Tsuda M, Saga Y (2007) Functional redundancy among Nanos proteins and a distinct role of Nanos2 during male germ cell development. *Development* 134:77–83.
16. Hay B, Ackerman L, Barbel S, Jan LY, Jan YN (1988) Identification of a component of Drosophila polar granules. *Development* 103:625–640.
17. Bardsley A, McDonald K, Boswell RE (1993) Distribution of tudor protein in the Drosophila embryo suggests separation of functions based on site of localization. *Development* 119:207–219.
18. Toyooka Y, et al. (2000) Expression and intracellular localization of mouse Vasa-homologue protein during germ cell development. *Mech Dev* 93:139–149.
19. Chuma S, et al. (2003) Mouse Tudor Repeat-1 (MTR-1) is a novel component of chromatoid bodies/nuages in male germ cells and forms a complex with snRNPs. *Mech Dev* 120:979–990.
20. Kedersha N, Anderson P (2007) Mammalian stress granules and processing bodies. *Methods Enzymol* 431:61–81.
21. Morita M, et al. (2007) Depletion of mammalian CCR4b deadenylase triggers elevation of the p27Kip1 mRNA level and impairs cell growth. *Mol Cell Biol* 27: 4980–4990.
22. Meyer S, Temme C, Wahle E (2004) Messenger RNA turnover in eukaryotes: Pathways and enzymes. *Crit Rev Biochem Mol Biol* 39:197–216.
23. Sada A, Suzuki A, Suzuki H, Saga Y (2009) The RNA-binding protein NANOS2 is required to maintain murine spermatogonial stem cells. *Science* 325:1394–1398.
24. Yuan L, et al. (2000) The murine SCP3 gene is required for synaptonemal complex assembly, chromosome synapsis, and male fertility. *Mol Cell* 5:73–83.
25. Cheng Y, et al. (2007) Abnormal sperm in mice lacking the Taf7l gene. *Mol Cell Biol* 27:2582–2589.
26. Ruggiu M, et al. (1997) The mouse Dazla gene encodes a cytoplasmic protein essential for gametogenesis. *Nature* 389:73–77.
27. Hayashi K, Yoshida K, Matsui Y (2005) A histone H3 methyltransferase controls epigenetic events required for meiotic prophase. *Nature* 438:374–378.
28. Sakai Y, Suetake I, Shinozaki F, Yamashina S, Tajima S (2004) Co-expression of de novo DNA methyltransferases Dnmt3a2 and Dnmt3L in gonocytes of mouse embryos. *Gene Expr Patterns* 5:231–237.
29. Aravin AA, et al. (2008) A piRNA pathway primed by individual transposons is linked to de novo DNA methylation in mice. *Mol Cell* 31:785–799.
30. Soyal SM, Amleh A, Dean J (2000) FIGalpha, a germ cell-specific transcription factor required for ovarian follicle formation. *Development* 127:4645–4654.
31. Choi Y, Ballow DJ, Xin Y, Rajkovic A (2008) Lim homeobox gene, lhx8, is essential for mouse oocyte differentiation and survival. *Biol Reprod* 79:442–449.
32. Rajkovic A, Pangas SA, Ballow D, Suzumori N, Matzuk MM (2004) NOBOX deficiency disrupts early folliculogenesis and oocyte-specific gene expression. *Science* 305: 1157–1159.
33. Kadyrova LY, Habara Y, Lee TH, Wharton RP (2007) Translational control of maternal Cyclin B mRNA by Nanos in the Drosophila germline. *Development* 134:1519–1527.
34. Wreden C, Verrotti AC, Schisa JA, Lieberfarb ME, Strickland S (1997) Nanos and pumilio establish embryonic polarity in Drosophila by promoting posterior deadenylation of hunchback mRNA. *Development* 124:3015–3023.
35. Boag PR, Atalay A, Robida S, Reinke V, Blackwell TK (2008) Protection of specific maternal messenger RNAs by the P body protein CGH-1 (Dhh1/RCK) during Caenorhabditis elegans oogenesis. *J Cell Biol* 182:543–557.
36. Gallo CM, Munro E, Rasoloson D, Merritt C, Seydoux G (2008) Processing bodies and germ granules are distinct RNA granules that interact in C. elegans embryos. *Dev Biol* 323:76–87.
37. Noble SL, Allen BL, Goh LK, Nordick K, Evans TC (2008) Maternal mRNAs are regulated by diverse P body-related mRNP granules during early Caenorhabditis elegans development. *J Cell Biol* 182:559–572.
38. Lee L, Davies SE, Liu JL (2009) The spinal muscular atrophy protein SMN affects Drosophila germline nuclear organization through the U body-P body pathway. *Dev Biol* 332:142–155.
39. Sheth U, Parker R (2003) Decapping and decay of messenger RNA occur in cytoplasmic processing bodies. *Science* 300:805–808.
40. Eulalio A, Behm-Ansmant I, Schweizer D, Izaurralde E (2007) P-body formation is a consequence, not the cause, of RNA-mediated gene silencing. *Mol Cell Biol* 27: 3970–3981.
41. Zheng D, et al. (2008) Deadenylation is prerequisite for P-body formation and mRNA decay in mammalian cells. *J Cell Biol* 182:89–101.
42. Knudson CM, Tung KS, Tourtellotte WG, Brown GA, Korsmeyer SJ (1995) Bax-deficient mice with lymphoid hyperplasia and male germ cell death. *Science* 270: 96–99.
43. Kanno J, et al. (2006) "Per cell" normalization method for mRNA measurement by quantitative PCR and microarrays. *BMC Genomics* 7:64.

BIOLOGY OF REPRODUCTION **84,** 734–742 (2011)
Published online before print 1 December 2010.
DOI 10.1095/biolreprod.110.087502

Endocrine Disrupter Bisphenol A Increases In Situ Estrogen Production in the Mouse Urogenital Sinus[1]

Shigeki Arase,[3,5] Kenichiro Ishii,[3,4,5] Katsuhide Igarashi,[6] Kenichi Aisaki,[6] Yuko Yoshio,[5] Ayami Matsushima,[7] Yasuyuki Shimohigashi,[7] Kiminobu Arima,[5] Jun Kanno,[6] and Yoshiki Sugimura[2,5]

Department of Nephro-Urologic Surgery and Andrology,[5] Mie University Graduate School of Medicine, Mie, Japan
Division of Cellular & Molecular Toxicology,[6] National Institute of Health Sciences, Tokyo, Japan
Laboratory of Structure-Function Biochemistry,[7] Department of Chemistry, Faculty of Sciences, Kyushu University, Fukuoka, Japan

ABSTRACT

The balance between androgens and estrogens is very important in the development of the prostate, and even small changes in estrogen levels, including those of estrogen-mimicking chemicals, can lead to serious changes. Bisphenol A (BPA), an endocrine-disrupting chemical, is a well-known, ubiquitous, estrogenic chemical. To investigate the effects of fetal exposure to low-dose BPA on the development of the prostate, we examined alterations of the in situ sex steroid hormonal environment in the mouse urogenital sinus (UGS). In the BPA-treated UGS, estradiol (E_2) levels and CYP19A1 (cytochrome P450 aromatase) activity were significantly increased compared with those of the untreated and diethylstilbestrol (DES)-treated UGS. The mRNAs of steroidogenic enzymes, *Cyp19a1* and *Cyp11a1*, and the sex-determining gene, *Nr5a1*, were up-regulated specifically in the BPA-treated group. The up-regulation of mRNAs was observed in the mesenchymal component of the UGS as well as in the cerebellum, heart, kidney, and ovary but not in the testis. The number of aromatase-expressing mesenchymal cells in the BPA-treated UGS was approximately twice that in the untreated and DES-treated UGS. The up-regulation of *Esrrg* mRNA was observed in organs for which mRNAs of steroidogenic enzymes were also up-regulated. We demonstrate here that fetal exposure to low-dose BPA has the unique action of increasing in situ E_2 levels and CYP19A1 (aromatase) activity in the mouse UGS. Our data suggest that BPA might interact with in situ steroidogenesis by altering tissue components, such as the accumulation of aromatase-expressing mesenchymal cells, in particular organs.

aromatase, bisphenol A, developmental biology, embryo, estradiol/estrogen receptor, in situ estrogen production, male reproductive tract, prostate, steroidogenic enzyme, urogenital sinus

INTRODUCTION

Endocrine-disrupting chemicals (EDCs) have been implicated in the alteration of fetal development of urogenital organs as well as the reproductive and endocrine systems in humans and other species [1]. The fetal development of urogenital organs is induced by endogenous hormonal messages that originate in fetal and maternal hormone systems. Fetal exposure to EDCs disrupts the interactions between endogenous hormones and their receptors, causing adverse effects later in life [2]. In the prostate, both androgens and estrogens play a significant role in development and differentiation as well as in the maintenance of adult homeostasis [3]. Therefore, even small changes in estrogen levels, including those of estrogen-mimicking chemicals, can lead to changes in prostate development and differentiation.

Bisphenol A (BPA), one of the EDCs, is a well-known, ubiquitous, estrogenic chemical used in the manufacture of polycarbonate plastics, as a lining in metal food and drink cans, and in dental sealants [4]. The concern with BPA originates from its detection in maternal and fetal plasma as well as the placenta [5, 6]. Thus, fetal exposure to BPA is implicated in fetal toxicity as well as in subsequent growth of the infant. Histopathologically, fetal exposure to low-dose BPA (10 μg kg^{-1} day^{-1}) has been shown to increase cell proliferation of urogenital sinus epithelium (UGE) in the primary prostatic ducts of CD1 mice [7]. Recently, our group reported that fetal exposure to low-dose BPA (20 μg kg^{-1} day^{-1}) specifically increased the number of basal epithelial cells in the adult prostate of BALB/c mice and also induced permanent cytokeratin 10 expression in such cells similar to the effects of synthetic estrogen diethylstilbestrol (DES; 0.2 μg kg^{-1} day^{-1}) [8]. Epigenetically, neonatal exposure of male rats to low-dose BPA (10 μg kg^{-1} day^{-1}) elicited critical molecular changes during prostate development and also increased prostatic gland susceptibility to precancerous neoplastic lesions and hormonal carcinogenesis [9]. Toxicological studies of BPA at less than 50 μg kg^{-1} day^{-1} in rodent fetuses and offspring have demonstrated alterations of mammary gland development, open-field behavior, and reproductive functioning [10–12].

Some EDCs are reported to alter the in situ sex steroid hormonal environment in the reproductive system. The triazine herbicide atrazine binds directly to adrenal-4-binding protein/steroidogenic factor-1 (official symbol NR5A1) and increases CYP19A1 (cytochrome P450 aromatase) expression and, ultimately, estradiol (E_2) production in human genital cancer cell lines [13]. The aryl hydrocarbon (dioxin) also increases CYP19A1 (aromatase) expression mediated by its receptor in mouse ovaries [14]. In contrast, the phosphorothioate insecticide profenofos increases the expression of steroidogenic genes

[1]Supported by Grants-in-Aid from the Ministry of Health, Labor, and Welfare, Japan. GEO accession no. GSE24928.
[2]Correspondence: Yoshiki Sugimura, Department of Nephro-Urologic Surgery and Andrology, Mie University Graduate School of Medicine, 2-174 Edobashi, Tsu, Mie 514-8507, Japan. FAX: 81 59 231 5203; e-mail: sugimura@clin.medic.mie-u.ac.jp
[3]These authors contributed equally to this work.
[4]Current address: Mie University Graduate School of Regional Innovation Studies, 1577 kurimamachiya-cho, Tsu, Mie 514-8507, Japan.

Received: 27 July 2010.
First decision: 19 August 2010.
Accepted: 15 November 2010.

eISSN: 1529-7268 http://www.biolreprod.org
ISSN: 0006-3363

and testosterone levels in rat testes [15]. Recently reported adverse effects of BPA on in situ steroidogenesis include increased testosterone levels in mouse Leydig cells and decreased E_2 levels in porcine ovarian granulosa cells [16, 17]. Thus, BPA may have the potential not only to mimic estrogenic action but also to alter in situ steroidogenesis in the prostate as well as other reproductive organs.

To investigate the effects of fetal exposure to low-dose BPA on in situ steroidogenesis in the developing prostate, we first measured sex steroid hormone levels and CYP19A1 (aromatase) activity in the BPA-treated mouse urogenital sinus (UGS), from which the prostate develops embryologically. Subsequently, we examined the alterations of steroidogenic enzyme gene expression to confirm the alterations of the in situ sex steroid hormonal environment in the BPA-treated mouse UGS. Finally, we identified the BPA-specific biological effects for in situ steroidogenesis during fetal prostate development.

MATERIALS AND METHODS

Animals

In the present study, 36 pregnant female C57BL/6 mice were purchased on the 12th day of gestation from Japan SLC, where the breeding strategy was to mate three female C57BL/6 mice (age, 10 wk) with one male overnight and separate them the next morning (plug date denoted as Day 0). All animals were housed individually in chip-bedded polyolefin cages in a room with controlled temperature (23 ± 1°C) and humidity (45 to 65%) on a 12L:12D photoperiod. Mice were fed a low-phytoestrogen diet (NIH-07PLD; Oriental Yeast Co.) and tap water ad libitum.

Chemicals

For the present study, both BPA and DES with a purity of 99% or greater were purchased from Nacalai Tesque and Wako Pure Chemical Industries, respectively.

Fetal Exposure to Chemicals

We randomly assigned 36 pregnant female C57BL/6 mice to three different treatment groups: BPA (20 μg kg^{-1} day^{-1}, n = 12) or DES (0.2 μg kg^{-1} day^{-1}, n = 12), both of which were dissolved in tocopherol-stripped corn oil (MP Biomedical, Inc.), administered by oral gavages on Embryonic Day (E) 13 to E16 and the control group, in which pregnant mice were fed tocopherol-stripped corn oil (2 ml/kg, n = 12). Previously, our group reported that this protocol of fetal exposure to BPA and DES resulted in similar histopathological changes of adult prostate—that is, increased basal epithelial cell number and induction of cytokeratin 10, a classic marker associated with squamous differentiation, in such cells [8]. Our dose level of BPA for the present study was also based on reported results suggesting that BPA is less than 100-fold less potent than DES. The Mie University's Committee on Animal Investigation approved the experimental protocol.

Termination and UGS Dissection

Between E17 and Postnatal Day (P) 1, all animals were terminated by an overdose of isoflurane followed by cervical dislocation. For each of the three groups, from 15 to 18 fetuses (both male and female) from three pregnant mice were collected at E17, E18, P0, and P1. The bladder and urethra were removed and dissected to isolate the UGS, and then the five or six UGS obtained were pooled as one sample. Thus, the 15–18 UGS were divided into three samples at each time point. The UGS, cerebellum, heart, kidney, testis, and ovary were collected in RNAlater (Applied Biosystems).

To isolate pure UGS, other tissues, such as the bladder, urethra, wolffian duct, seminal vesicle, and mullerian duct, were removed from both the male and female urogenital tracts. The histopathology of the mouse UGS was then examined by hematoxylin-and-eosin staining.

Measurements of In Situ E_2 Levels and CYP19A1 (Aromatase) Activity in UGS

The E_2 levels and CYP19A1 (aromatase) activity in UGS were determined by liquid chromatography-tandem mass spectrometry [18] and a tritiated water release assay [19], respectively, which were made available by Aska Pharma Medical. Briefly, the organs were homogenized, and the extracts were applied to a C18 Amprep solid-phase column (Amersham Biosciences) to remove contaminating fats. The E_2 was then separated using a normal-phase high-performance liquid chromatography system (Jasco) with a silica gel column (Cosmosil 5SI; Nacalai Tesque), and 100 pg of isotope-labeled [$^{13}C_4$]E_2 were added to extracts. The evaporated extracts were reacted with 5% pentafluorobenzyl bromide/acetonitrile, under KOH/ethanol, for 1 h at 55°C. After evaporation, the products were reacted with 100 ml of picolinic acid solution (2% picolinic acid, 2% 2-dimethylaminopyridinc, and 1% 2-methyl-6-nitrobenzoic acid in tetrahydrofuran) and 20 ml of triethylamine for 0.5 h at room temperature. The reaction products were dissolved in 1% acetic acid and then purified using a Bond Elute C18 column (Varian). The products were measured with a reverse-phase liquid chromatograph (Agilent 1100; Agilent Technologies) coupled with an API 5000 triple-stage quadrupole mass spectrometer (Applied Biosystems) in the positive-ion mode. This device monitored the *m/z* 558 to *m/z* 339 (E_2) and *m/z* 562 to *m/z* 343 ([$^{13}C_4$]E_2) transitions.

The tritiated water release assay was used for the measurement of CYP19A1 (aromatase) activity. This method measures the production of ^3H_2O, which forms as a result of aromatization of the substrate [1b-^{3}H]androst-4-ene-3,17-dione (New England Nuclear). Serum-free medium containing [1b-^{3}H]androst-4-ene-3,17-dione solution (54 nM) was prepared, of which 0.5 ml was added to each sample. After incubation for 1 h, the samples were placed on ice, and 200 μl of culture medium were withdrawn. The medium was extracted with 500 μl of chloroform, vortexed, and then centrifuged for 1 min at 9000 × *g*. A 100-μl aliquot of the aqueous phase was mixed with 100 μl of a 5% (wt/vol) charcoal/0.5% (wt/vol) dextran T-70 suspension, vortexed, and then incubated at room temperature for 10 min. Then, after centrifugation of the solution for 5 min at 9000 × *g*, a 150-μl aliquot was removed for measurement of radioactivity by liquid scintillation.

RNA Extraction and cDNA Preparation

Total RNA was extracted using the RNeasy Mini Kit (Qiagen, Inc.) in accordance with the manufacturer's instructions. The RNA concentration was then determined spectrophotometrically by a multidetection microplate reader (Dainippon Sumitomo Pharma Co.). From 50 ng of total RNA, cDNA was reverse transcribed using oligo(dT) and Superscript II RNase H-reverse transcriptase (Invitrogen) as previously described [8].

Analysis of Gene Expression Profile

For determining gene expression profiles of the male UGS, GeneChip analysis with the Percellome method was performed [20]. Briefly, organs were prepared using RLT buffer (Qiagen, Inc.). Total RNA was extracted using RNeasy Mini Kit. First-strand cDNA was synthesized by incubating 5 mg of total RNA with a T7 oligo(dT) primer (Invitrogen) according to the manufacturer's protocol. The dsDNA was mixed with T7 RNA polymerase (Enzo Biochem, Inc.). During the in vitro transcription, generated cRNAs were labeled with biotin-16-UTP and biotin-11-CTP (Enzo Biochem, Inc.). The purified cRNA was fragmented at 300–500 bp into the target solution. Hybridization was performed with the GeneChip Mouse Genome 430 Version 2.0 (Affymetrix, Inc.) at 45°C for 18 h after staining with streptavidin-R-phycoerythrin conjugates (Molecular Probes, Invitrogen). The reacted arrays were then scanned as digital image files, and the scanned data were analyzed with GeneChip Operating Software (Affymetrix, Inc.). The expression data were converted to copy numbers of mRNA per cell by the Percellome method, quality controlled, and analyzed using Percellome software [20].

Real-Time PCR Analysis

Real-time PCR was carried out in the iCycler iQ Detection System (Bio-Rad Laboratories) with iQ SYBR-Green Supermix reagents (Bio-Rad Laboratories) as previously described [8]. The PCR amplification reaction was performed with specific primers as shown in Table 1. After PCR, melting-curve analysis was performed to verify specificity and identity of the PCR products. All data were analyzed with the iCycler iQ Optical System Software Version 3.0A (Bio-Rad Laboratories). All PCR data were normalized to *Gapdh* mRNA.

Preparation of Primary Cultured Mesenchymal Cells from UGS

The UGS were dissected from the fetuses and separated into UGE and urogenital sinus mesenchyme (UGM) by tryptic digestion and mechanical separation as previously described [21]. UGM were cultured in RPMI-1640

TABLE 1. Sequences of oligonucleotide primers used for the real-time PCR analyses.

Gene	Primer[a]
Gapdh	F: 5′-AAATGGTGAAGGTCGGTGTG-3′
	R: 5′-TGAAGGGGTCGTTGATGG-3′
Cyp19a1	F: 5′-GCCCAATGAATTTACCCTCGAA-3′
	R: 5′-AAGCCAAAAGGCTGAAAGTACCT-3′
Cyp11a1	F: 5′-TCGACTCCTCAGAACTAAGACCTG-3′
	R: 5′-GTACCCTGGTGTCCTTTATAGCCT-3′
Nr5a1	F: 5′-CCTGGGCTGGCTACCTCTATC-3′
	R: 5′-CGAACTAGAGCCAGAGGAGGAC-3′
Esr1	F: 5′-GCACAGGATGCTAGCCTTGTCTC-3′
	R: 5′-AATTGTCACCAGCTTGCAGGTTC-3′
Ar	F: 5′-GGCGGTCCTTCACTAATGTCAACT-3′
	R: 5′-CTGACTTGTGCATGCGGTACTCAT-3′
Esrrg	F: 5′-CCGAGAGTTGGTGGTTATCATTGG-3′
	R: 5′-GGAAGACCCTCGCCGTGC-3′

[a] F, forward; R, reverse.

with 5% fetal bovine serum and plated out on four-well glass slides (BD Falcon). After several days, cells were fixed in methanol and processed for immunocytochemical analysis.

Immunocytochemical Staining

The sections were first incubated for 15 min in 0.01 M PBS. After inhibition of endogenous peroxidases (10 min in 0.6% H_2O_2 diluted in 0.01 M PBS plus 0.2% Triton X-100 [PBST]) and saturation (2 h in a 5% normal goat serum solution), sections were incubated overnight at 4°C in a polyclonal affinity-purified antiaromatase antibody or estrogen-related receptor gamma (ESRRG) antibody raised in rabbit against quail recombinant aromatase or ESRRG diluted 1:500 in 0.01 M PBST. The next day, the sections were immersed for 2 h at room temperature in a biotin-conjugated goat anti-rabbit immunoglobulin G (DakoCytomation, Inc.) diluted 1:400 in PBST and then for 2 h in a streptavidin-fluorescein complex (Rhodamine; DakoCytomation, Inc.) diluted 1:50 in PBST. Between each step, sections were extensively rinsed in PBST. The sections were mounted onto microscope slides, coverslipped with a gelatin-based mounting medium, and stored in the dark at 4°C. For double-labeling immunofluorescence, Alexa Fluor 488- or 594-conjugated secondary antibodies were used. Rabbit polyclonal anti-aromatase antibody was kindly provided by Prof. Nobuhiro Harada (Department of Biochemistry, Fujita Health University School of Medicine, Aichi, Japan) [22]. The rabbit polyclonal anti-ESRRG antibody used in the present study was established and characterized as previously reported [23]. The mouse monoclonal anti-Ran antibody (Santa Cruz Biotechnology, Inc.) was used to detect nucleus in cells. Ran, also called TC4, is the small RAS-related protein that is localized in the nucleus.

Statistical Analysis

Results are expressed as the mean ± SD. Differences among the three groups were determined using Student *t*-test with Dunnett multiple comparison. A value of $P < 0.05$ was considered to be statistically significant.

RESULTS

BPA-Specific Increases of E_2 Levels and CYP19A1 (Aromatase) Activity in Mouse UGS

The pregnant mice were exposed to low-dose BPA during the onset of prostatic budding (E13–E16), and the UGS of fetuses were collected during bud elongation (E17–P1). In analyses of in situ sex steroid hormonal environment, E_2 levels and CYP19A1 (aromatase) activity were significantly increased only at P1 in BPA-treated UGS, not at P1 in the DES-treated UGS (Fig. 1). At E17 and P1, both the E_2 levels and CYP19A1 (aromatase) activity in untreated male UGS were not significantly different compared with those in untreated female UGS.

BPA-Specific Up-Regulation of Steroidogenic Enzyme and Sex-Determining Gene mRNA in Mouse UGS

To investigate the BPA-specific gene alterations related to increases of the E_2 levels and aromatase activity, we performed preliminary GeneChip analysis with the Percellome method in the BPA- or DES-treated male UGS at E17 and P1. The results showed BPA-specific mRNA up-regulation of steroidogenic enzymes, such as *Cyp11a1*, *Cyp11b1*, and *Cyp17a1*, and sex-determining factors, such as *Nr5a1*, *Nr0b1*, *Gata4*, and *Amhr2* (data not shown). Furthermore, quantitative PCR analysis confirmed the mRNA up-regulation of *Cyp19a1*, *Cyp11a1*, and *Nr5a1* only in the BPA-treated neonatal (P0 and P1) UGS, not in the DES-treated neonatal UGS (Fig. 2). No difference in mRNA expression levels was found between E17 and P1 when comparing the untreated male UGS to that of the female. In

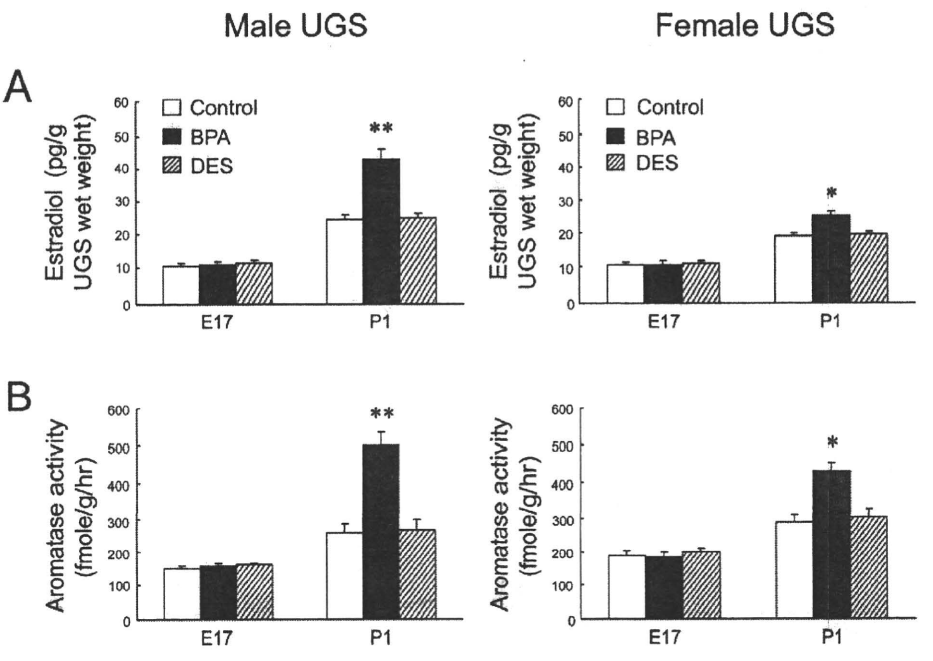

FIG. 1. BPA-specific increases of E_2 levels and CYP19A1 (aromatase) activity in mouse UGS. E_2 levels (**A**) and CYP19A1 (aromatase) activity (**B**) were measured in the untreated control (open bar), BPA-treated UGS (closed bar), and DES-treated UGS (slashed bar) at E17 and P1. $*P < 0.01$, $**P < 0.001$ vs. control.

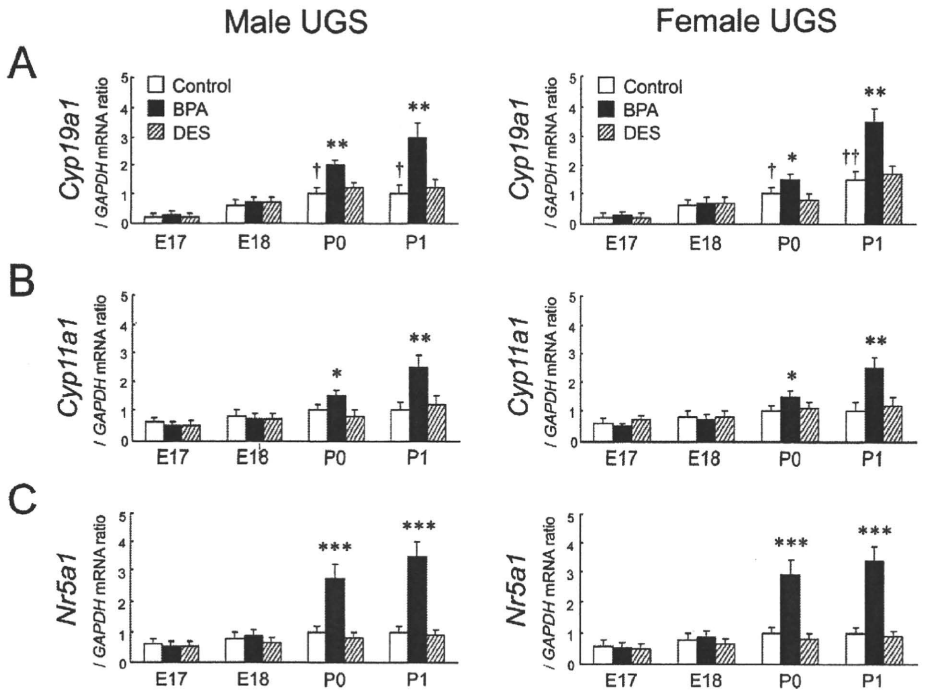

FIG. 2. BPA-specific up-regulation of steroidogenic enzyme and sex-determining gene mRNA in mouse UGS. The relative mRNA expressions of *Cyp19a1* (**A**), *Cyp11a1* (**B**), and *Nr5a1* (**C**) were determined in the untreated control (open bar), BPA-treated UGA (closed bar), and DES-treated UGS (slashed bar) between E17 and P1. $^{*}P < 0.05$, $^{**}P < 0.01$, $^{***}P < 0.001$ vs. control at each time point; $^{\dagger}P < 0.01$, $^{\dagger\dagger}P < 0.001$ vs. control at E17.

untreated male and female UGS, the mRNA of *Cyp19a1* was gradually increased between E17 and P1.

Restricted BPA-Specific Up-Regulation of Steroidogenic Enzyme and Sex-Determining Gene mRNA in UGE and UGM

In male fetuses at P1, it was not feasible to separate UGE and UGM components within the male UGS because of the formation of prostatic buds. In the female at P1, the up-regulation of *Cyp19a1*, *Cyp11a1*, and *Nr5a1* mRNA was observed only in UGM, not in UGE, of the BPA-treated group (Fig. 3). In both male and female UGE, expressions of such mRNAs were quite low and not up-regulated, even in the BPA-treated group. At E17, no difference in mRNA expression levels was found when comparing the untreated male UGM with that of the female.

BPA-Specific Increases of Aromatase-Expressing Cells in Primary Cultured UGM

In both the male and female, P1 UGM was primary cultured in vitro. Representative pictures of aromatase-positive cells are shown in Figure 4, A–C. The aromatase-positive staining was

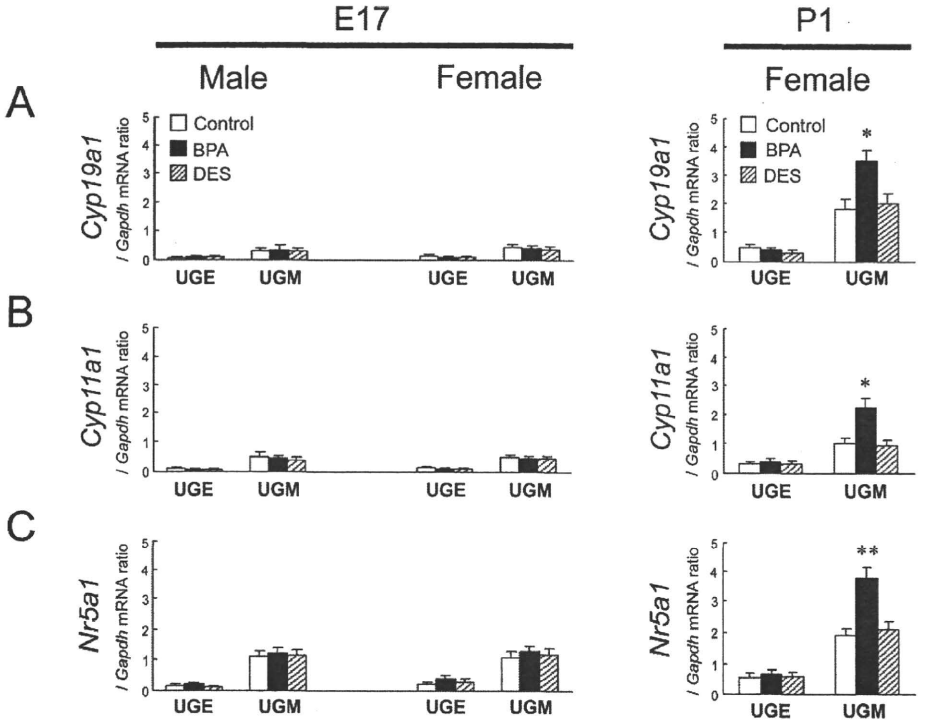

FIG. 3. Restricted BPA-specific up-regulation of steroidogenic enzyme and sex-determining gene mRNA in UGE and UGM. The relative mRNA expressions of *Cyp19a1* (**A**), *Cyp11a1* (**B**), and *Nr5a1* (**C**) were determined for UGE and UGM of the untreated control (open bar), BPA-treated UGS (closed bar), and DES-treated UGS (slashed bar) at E17 and P1. $^{*}P < 0.01$, $^{**}P < 0.001$ vs. control.

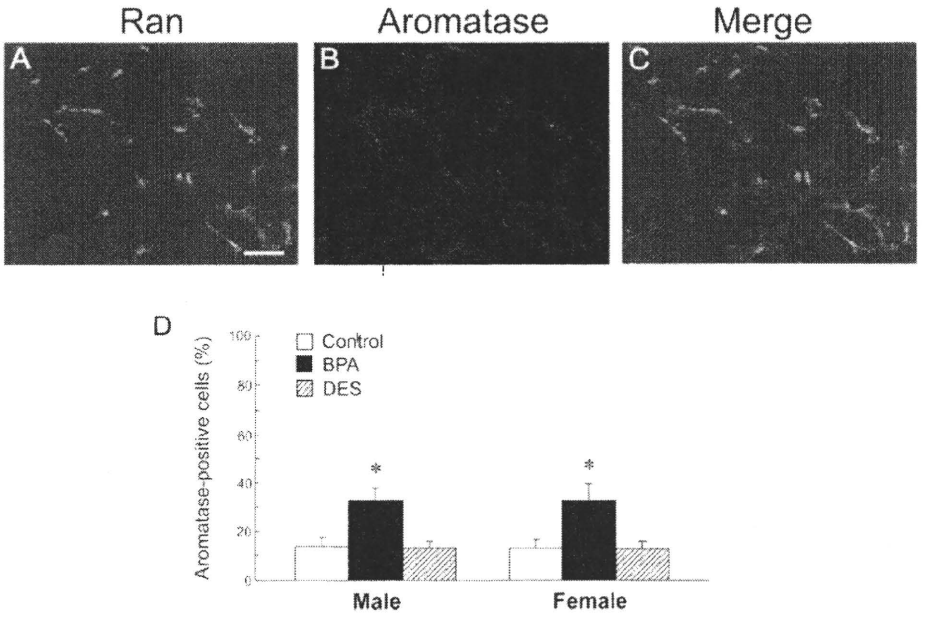

FIG. 4. BPA-specific increases of aromatase-expressing cells in primary cultured UGM. **A–C**) Fluorescence signals were detected for the CYP19A1 (aromatase) protein in primary cultured UGM. The nuclei were identified by Ran staining. Bar = 100 μm, magnification ×400. **D**) The number of aromatase-positive cells was counted in primary cultured UGM of the untreated control (open bar), BPA-treated UGS (closed bar), and DES-treated UGS (slashed bar), and the percentage of aromatase-positive cells was calculated from at least 10 areas. $^{*}P < 0.01$ vs. control.

observed in the cytoplasm of cultured UGM. The rate of positivity (i.e., the percentage of cells that expressed CYP19A1 [aromatase] protein), was approximately 10% in the untreated and the DES-treated groups, whereas it was as high as approximately 30% in the BPA-treated group (Fig. 4D). No difference in the rate of positivity of CYP19A1 (aromatase) was found when comparing the untreated male UGM to that of the female.

Restricted BPA-Specific Up-Regulation of Esrrg *mRNA in UGE and UGM*

In E17 female UGM, the mRNA expression of *Esr1* was up-regulated by both BPA and DES treatment (Fig. 5A). At E17, however, the mRNA expression of *Ar* was up-regulated by both BPA and DES treatment in the male UGS (Fig. 5B). At P1, mRNA expression of *Ar* was up-regulated by both BPA and DES treatment in the female UGS (Fig. 5B). In both the male and female, the up-regulation of *Esrrg* mRNA was observed at E17 and restricted in UGM, but not in UGE, of the BPA-treated group (Fig. 5C). In both the male and female UGE, the expression of *Esrrg* mRNA was quite low and not up-regulated, even in the BPA-treated group. At E17, no difference in mRNA expression levels was found when comparing the untreated male UGS with that of the female.

BPA-Specific Increases of ESRRG-Expressing Cells in Primary Cultured UGM

In both the male and female, E17 UGM was primary cultured in vitro. Representative pictures of ESRRG-positive

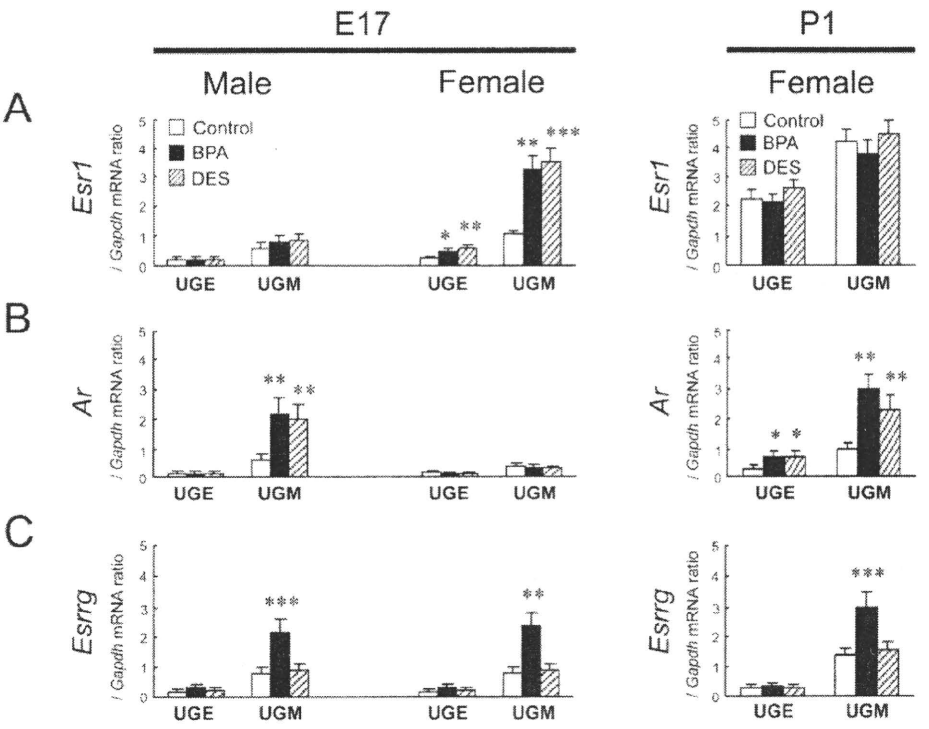

FIG. 5. Restricted BPA-specific up-regulation of *Esrrg* mRNA in UGE and UGM. The relative mRNA expressions of *Esr1* (**A**), *Ar* (**B**), and *Esrrg* (**C**) were determined in UGE and UGM of the untreated control (open bar), BPA-treated UGS (closed bar), and DES-treated UGS (slashed bar) at E17 and P1. $^{*}P < 0.05$, $^{**}P < 0.01$, $^{***}P < 0.001$ vs. control.

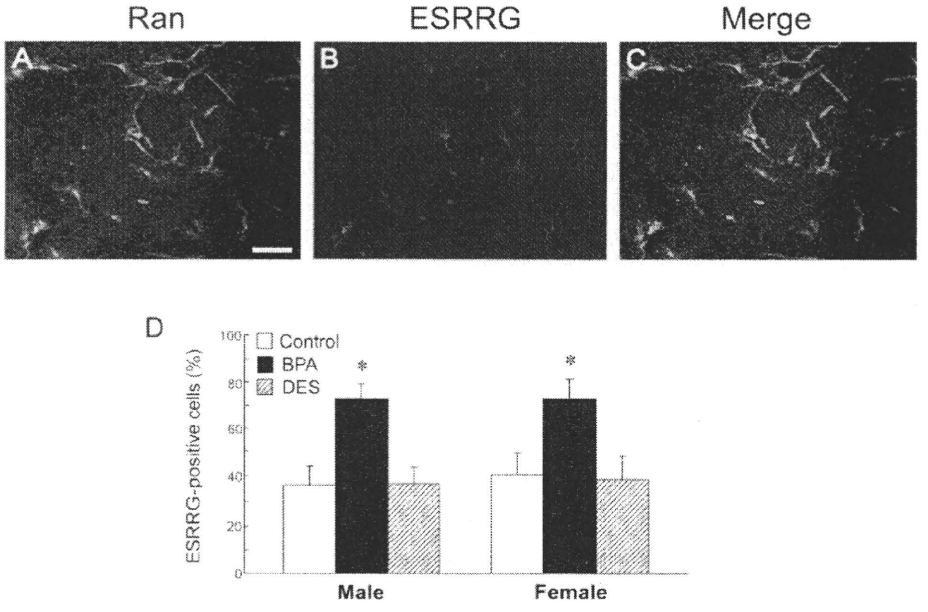

FIG. 6. BPA-specific increases of ESRRG-expressing cells in primary cultured UGM. **A–C**) Fluorescence signals were detected for the ESRRG protein in primary cultured UGM. The nuclei were identified by Ran staining. Bar = 100 μm, magnification ×400. **D**) The number of ESRRG-positive cells was counted in primary cultured UGM of the untreated control (open bar), BPA-treated UGS (closed bar), and DES-treated UGS (slashed bar), and the percentage of ESRRG-positive cells was calculated from at least 10 areas. $^*P < 0.01$ vs. control.

cells are shown in Figure 6, A–C. The ESRRG-positive staining was observed in both the nucleus and the cytoplasm of cultured UGM. The number of ESRRG-positive UGM was significantly increased only in the BPA-treated group and showed a 2.2-fold increase in males and a 1.6-fold increase in females (Fig. 6D). No difference was found in the rate of positivity of ESRRG when comparing the untreated male UGM with that of the female.

BPA-Specific Up-Regulation of Esrrg *and Steroidogenic Enzyme mRNA in Sex Hormone-Related Organs*

To investigate the BPA-specific up-regulation of in situ steroidogenesis in other organs, we first examined the changes in *Esrrg* mRNA expression in sex hormone-related organs, such as the cerebellum, heart, kidney, ovary, and testis. At P1, the mRNA expression of *Esr1* in the cerebellum, heart, kidney, and ovary, but not in the testis, was up-regulated by both BPA and DES treatment (Fig. 7A). However, no significant difference in *Ar* mRNA expression was observed in all organs examined (Fig. 7B). In the untreated group, the mRNA expression of *Esrrg* was not detected in the testis at E17 and P1 (Fig. 7C). The up-regulation of *Esrrg* mRNA was observed at E17 and restricted to the cerebellum, heart, kidney, and ovary (Fig. 7C). The BPA-specific up-regulation of *Cyp19a1*, *Cyp11a1*, and *Nr5a1* mRNA was observed only at P1 in the cerebellum, heart, kidney, and ovary, but not in the testis (Fig. 8).

DISCUSSION

Concern about the effects of EDCs such as BPA on human health has been increasing [24]. Although the majority of EDCs have the potential to alter functioning of the reproductive and endocrine system, the actual mechanism responsible for such alterations has not been identified thoroughly. BPA is of concern because its chemical structure resembles that of DES. Several studies have reported that BPA can mimic estrogen action, such as induction of vaginal cornification, uterine vascular permeability, growth and differentiation of the mammary gland, and synaptic plasticity in the hippocampus [25–28]. In the prostate, alterations in normal development can produce permanent changes that persist throughout adulthood and may increase the risk of disease in later life [9]. Thus, our objective was to investigate the biological effects of low-dose BPA on the initial development of primary ducts in the fetal prostate.

During prostatic development, alteration of sex steroid hormone synthesis may be responsible for prostatic anomalies associated with fetal exposure to EDCs. In the present study, fetal exposure to low-dose BPA increased E_2 levels in P1 UGS of both the male and female, whereas DES-induced changes were not detected. This alteration was also correlated with increased activity of CYP19A1 (aromatase) in UGS at P1, suggesting the unique action of BPA for in situ steroidogenesis in UGS. The BPA-specific increase of E_2 levels in UGS at P1 was correlated with the following: mRNA up-regulation of steroidogenic enzymes, such as *Cyp19a1* and *Cyp11a1*, and an increased number of aromatase-expressing UGM. The enzyme CYP19A1 (aromatase) is responsible for in situ E_2 production and the crucial testosterone/E_2 balance necessary for normal embryonic and fetal development, even in males. The data presented here shows that the up-regulation of *Cyp19a1* mRNA in BPA-treated UGM was comparable to changes in both in situ E_2 production and CYP19A1 (aromatase) activity.

In the present study, we demonstrated that the BPA-specific increase in steroidogenic enzyme mRNA and aromatase-expressing cell number were observed in both the male and female UGM. During embryonic development, the mesenchymal component is involved in the induction and organogenesis of various organs, including the prostate, mammary gland, lung, kidney, and pancreas. It has been well established that subpopulations of the mesenchymal component are a source of potent molecules that regulate epithelial growth and differentiation [29]. In the prostate, androgen-responsive signals derived from UGM permissively and instructively induce UGE to form primary ducts of the prostate [30].

Comparison between the neonatal male and female UGS shows a similarity in the condensed mesenchyme of the ventral areas—that is, the ventral prostate mesenchyme (VPM) in the male and the ventral mesenchymal pad (VMP) in the female [31]. In the male, a defined VPM is specifically associated with ductal branching morphogenesis and cytodifferentiation of the ventral prostate. Females do not usually form a prostate. In a